Chapter 3
Recent Advances in Hybrid Supercapacitors

T. Manovah David and Tom Mathews

Contents

Abstract Research on electrochemical storage systems are persistently on the rise especially in the fields of supercapacitors and batteries. Several modifications are made continuously in supercapacitors with an intention to retain its excellent power density and to improve the inherently poor energy density. Initially, changes were made to these systems by introducing new electrodes, then new materials such as pseudocapacitors were launched and recently the formation of 'hybrid' systems.

T. M. David · T. Mathews (✉)
Thin Films and Coatings Section, Surface Nanoscience Division, Materials Science Group, Indira Gandhi Centre for Atomic Research, Kalpakkam, Tamil Nadu, India
e-mail: tom@igcar.gov.in

Three predominant supercapacitor hybrid systems are reported so far viz. symmetric, asymmetric, and supercapacitor-battery hybrid (SBH) systems. Each amendment in the hybrid systems revolutionized the electrochemical storage systems; however, the SBH systems dominated all the forms of hybrid devices. Several battery electrodes are introduced in hybrid cell along with a supercapacitor electrode and they exhibit excellent energy densities at high power densities. This chapter briefly reviews all forms of hybrid supercapacitors.

Keywords Hybrid supercapacitor · Symmetric electrodes · Asymmetric electrodes · Supercapattery · EDLC · Pseudocapacitance

3.1 Introduction

One of the greatest concerns for the global society is materials for high performance energy storage in unique devices. Several energy storage materials are well known to the scientific and the commercial community. Some have excellent energy densities viz., nickel-metal hydride batteries, nickel-cadmium batteries and lithium-ion batteries (LIBs). On the other hand, some have superior power densities, such as supercapacitors. Interestingly, both forms of energy storage systems are novel, eco-friendly, economic, and exhibit greater performance. Also, they have the ability to meet the need of the ever-increasing global demand. The comparison of the energy densities and power densities of both batteries and capacitors are given in Table 3.1. In spite of all the grand and impending abilities of these materials, they are yet incompetent and fall short of their expectations, when they are used as batteries and supercapacitors individually, with the possibility of non-monotonic consumption of energy occurring as a result of frequent modifications during the battery discharging processes (Kouchachvili et al. 2018). With these hitches, several modifications in the energy components have been tried to make the balance right, that is, to improve both the densities (energy and power) without compromising each other.

Major work is going on in the sectors of batteries and supercapacitors. Especially, in the supercapacitor sector the scientists are looking forward to harness its power density along with improvement in the energy density. For this purpose, several electrode materials have been tested such as having electrical double layer capacitance (EDLC) electrodes and pseudocapacitance with improved energy density with innate power density. But the progress was stalled after a certain limit without the possibility of moving any further. Therefore, the researchers have implemented the

Table 3.1 Comparison of lithium-ion batteries and supercapacitors

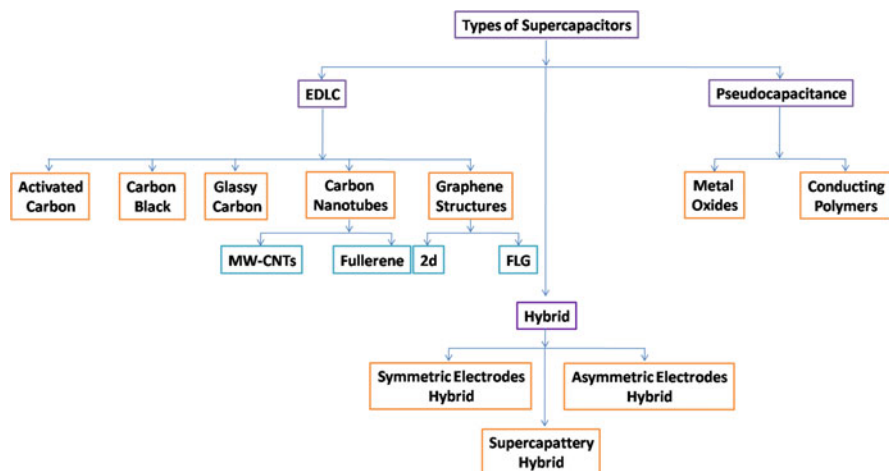| Devices	Parameters		
	Energy density (Wh kg^{-1})	Power density (kW kg^{-1})	Cycles
Supercapacitor	5–10	10	>1 $\times$ 10^5
Li-ion battery	150–200	1	<1000

Fig. 3.1 Classifications of the supercapacitors. Electric double layer capacitance (EDLC), multiwall carbon nanotubes (MW-CNTs), two dimensional (2d), few layer graphene (FLG)

idea of combining two different electrodes to fabricate a supercapacitor with enhanced energy density. The classification of supercapacitors is given in Fig. 3.1.

The combination of two distinct electrodes in a single unit has led to the formation of hybrid supercapacitors. Hybrid supercapacitors are systems with enhanced energy density along with improved power density. Three different types of hybrid supercapacitors are now reported viz.: (a) symmetric hybrid supercapacitors, (b) asymmetric hybrid supercapacitors, and (c) supercapacitor-battery hybrid (SBH). A simple definition of a hybrid capacitor is that it may be two different electrodes (asymmetric) or same electrodes made with hybrid composites (symmetric) or a combination of a supercapacitor electrode and a battery electrode (Chen et al. 2010). The electrodes can be exhibiting electric double layer capacitance (EDLC) or pseudocapacitance behavior or can also be a battery electrode. In other words, one half is constituted of EDLC and the other half with pseudocapacitance electrode or one of these supercapacitor electrodes on one side and the battery electrode on the other (Muzaffar et al. 2019). The combined properties are said to have a positive effect on the assembled hybrid supercapacitor. For example, in a EDLC and pseudocapacitance hybrid, the former electrode displays intrinsic charge storage based on double layer formation depending on the atomic charge partition length and the later is based on repetitive redox reactions (Lu et al. 2011). The amalgamation of these electrodes as anodes and cathodes constitutes a hybrid capacitor.

The energy storage ability of hybrid supercapacitors is better as identified in the Ragone plot (power density [W kg^{-1}] vs. energy density [Wh kg^{-1}]) when compared with other such similar devices such fuel cells, batteries, non-hybrid supercapacitors such as EDLC and pseudocapacitor and conventional capacitors (Fig. 3.2). The hybrid supercapacitors have an edge over other energy storage

Fig. 3.2 Ragone plot for different energy storage devices. The plot compares the specific energy and power of electrical double layer (EDL) supercapacitor, supercapattery, internal combustion engine, rechargeable battery and redox flow battery and fuel cell. (Reprinted with permission of Taylor and Francis from Chen 2017)
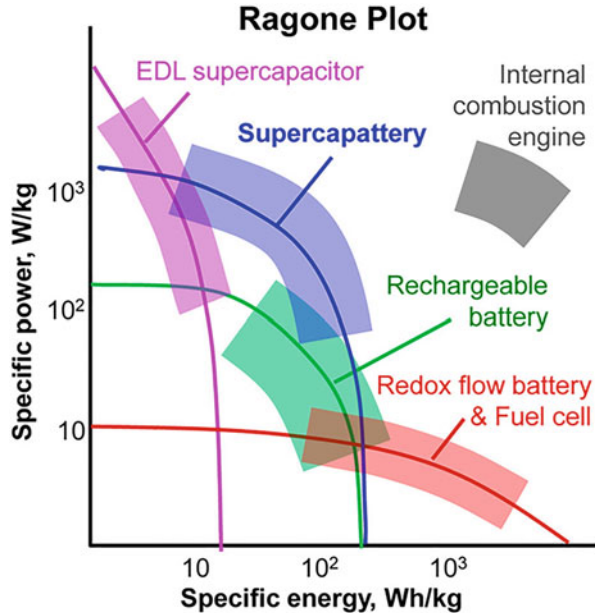

systems. The plot also gives information that all the types of supercapacitors have better power density over the present rechargeable batteries. This phenomenon of large power density is largely possible because only the outer surface of the supercapacitors is used whereas in batteries, processes like intercalation and de-intercalation takes place (Lee et al. 2011). On the other hand, hybrid supercapacitors exhibit large storage ability with superior power rates. This capability of hybrid supercapacitors makes them a suitable choice to replace portable batteries used in mobile phones where both high energy and power densities could be utilized along with improvement in the net cell voltage (Jorio et al. 2001; Plitz et al. 2006). This unique combination of higher power density along with higher specific energy defines the possibility of using the hybrid supercapacitor as a complement to most of the other power sources (Pandolfo and Hollenkamp 2006).

The credentials of hybrid supercapacitors are found to be superior. A good understanding in every aspect of this is required and this chapter reviews the basic construction of a supercapacitor cell, type of electrical energy storage in supercapacitors, hybrid supercapacitors and their various forms.

3.2 Construction of a Supercapacitor Cell

The supercapacitor assembly is very much similar to that of a conventional battery system where both the electrodes are inserted into an electrolyte. The major difference of supercapacitors from that of batteries is that both the electrodes are separated

by an ion-permeable membrane, meaning that the electrodes are separated by a membrane. However, the electrodes of a battery are not separated by an ion-permeable membrane. For better understating the electrode/electrolyte *interface* is considered to be one *capacitor*. Therefore, when a supercapacitor cell is constructed, it means that two capacitors (each electrode) in series separated by an electrolyte resistance. The general equivalent electrical circuit for a symmetrical capacitor cell is given as,

$C_{dl(a)}$ R_s $C_{dl(c)}$
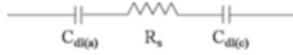
where, the $C_{dl(a)}$ and $C_{dl(c)}$ are double layer capacitance of anode and cathode, respectively, and R_s is the electrolyte resistance exerted.

The capacitance of the supercapacitor cell (C_{cell}) is given as (Winter and Brodd 2004),

$$1/C_{cell} = 1/C_{dl(a)} + 1/C_{dl(c)} \qquad (3.1)$$

If $C_{dl(a)} = C_{dl(c)}$, then eq. (3.1) could be written as

$$C_{cell} = C_{dl(a)}/2 \qquad (3.2)$$

Then, the double layer capacitor is given to be as,

$$C_{dl} = \varepsilon A/4\pi d \qquad (3.3)$$

where ε is the dielectric constant of the electrical double layer formed, A denotes the surface area, and d is thickness of the double layer (Qu and Shi 1998). Higher capacitance can be achieved based on the formulae, when the charge separation is thin and surface area is large. The information helps in deriving the energy and power densities of the capacitor,

$$E = CV^2/2 \text{ or } QV/2 \qquad (3.4)$$

$$P = V^2/4R \qquad (3.5)$$

where E is energy, C is capacitance, V is applied voltage, Q is charge, P is power density, and R is resistance (Conway 2013).

Apart from the formulae, two other factors are involved in deciding the efficacy of a supercapacitor material viz. (a) the pore-size distribution and (b) operating voltage. The pore-size distribution plays a pivotal role in directing the ion movement in the electrode within the pores since ions cannot travel in solids as in liquids. The ionic movement is largely hindered if the pore-size is extremely small and, therefore, can never contribute to the capacitance. If the size of pores is very less, then the

capacitance achieved and the specific surface area will not match (Sharma and Bhatti 2010). Moreover, another important factor determining the capacitance is the size of the ions. Smaller the ions in the electrolyte greater the capacitance. Also, a pivotal role is played by the operating voltage that is determined by the electrolyte. It is a deciding factor for the specific energy and power density of the supercapacitors. Usually aqueous electrolytes such as acidic or basic solutions H_2SO_4 or KOH, respectively, have a poor decomposition voltage of around ~1.23 V (Fernández et al. 2008). Non-aqueous electrolytes or organic electrolytes such as acetonitrile and propylene carbonate improve the operating voltage up to 2.5 V (Du et al. 2013).

3.3   Electrical Energy Storage in Different Types of Supercapacitors

Generally, the supercapacitors involve two different types of energy storage mechanisms. They are electrical double layer capacitance (EDLC) and the pseudocapacitance involving redox reactions. The EDLC type does not have electrochemically active electrodes and, therefore, no transfer of electrons take place at the electrode–electrolyte interface. The charges are stored in EDLC electrostatically and this type is also known as non-Faradaic charge storage. An example for EDLC type charge storage electrode is Carbon. On the other hand, electrode materials with electrochemically active (transferring electrons) property display pseudocapacitance. In this type, the electrons are transferred across the interface and this process is known as *Faradaic* charge storage. For better understanding all the major classification of supercapacitors is described here viz. EDLC, pseudocapacitance, and hybrid supercapacitor.

3.3.1   Electric Double Layer Capacitor

As a charged material such as carbon electrode is dipped into an electrolyte, electric double layer capacitance (EDLC) arises. When the electrode is dipped a swift arrangement of a double layer takes place. The accumulation of charges is like electrons or holes in the electrode and the respective counter-ions in the electrolyte. In other words, there is adsorption of ion on the surface of the electrode. The EDLC type charge storage is very common and several theories have been put forward to explain the double layer formation as shown in Fig. 3.3. The very simple model is called the Helmholtz model (Fig. 3.3a), where the charges are accumulated continuously along the electrode. Here the theory considers the formation of rigid layer, which counterbalances the charges formed in the solid (Endo et al. 2001). This is also called approximation modeling. Thereafter, Gouy-Chapman (Fig. 3.3b) came up with another theory with the introduction of diffuse layer. This theory states that
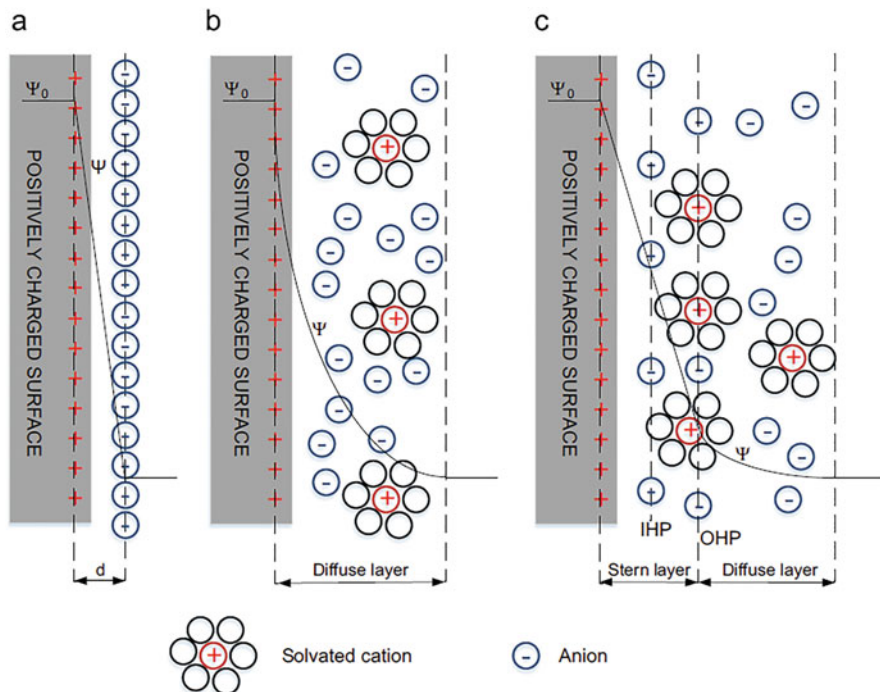
Fig. 3.3 Electrical double layer capacitance (EDLC) models (**a**) Helmholtz model, (**b**) Gouy-Chapman model and (**c**) Stern model. (Reprinted with permission of Elsevier from González et al. 2016). The terms IHP and OHP in the image indicates inner Helmholtz layer and outer Helmholtz layer, respectively

the ions in the solution tend to diffuse into the liquid phase until a counter potential is set. In addition, the kinetics of movement of the ions will also determine the diffusion of the ions (González et al. 2016). The theory could not explain much as the diffusion layer was thicker than the theoretically devised one. Finally, Stern devised another theory (Fig. 3.3c) with two adjacent layers in one diffusion layer. That is, one of the layers is compact and it is closer to the electrode known as inner Helmholtz layer. The layer away from the electrode is known as outer Helmholtz layer [or Gouy-Chapman layer] (Zhang and Zhao 2009). This theory clarified the formation of EDLC in supercapacitors.

In this type of supercapacitors, when a cell is constructed, both the electrodes contribute individually to the formation of electric double layer capacitance (EDLC). One of the electrodes will have an excess of electrons and other will have a deficiency of electrons (Fig. 3.4). The applied potential between the anode and cathode strictly direct the accumulation and withdrawal of electrons over electrodes. The arrangement takes place in such a manner that the status of the electrode is maintained at electroneutrality at the interface. Therefore, this process involved only the surface of the electrode for charge storage, and hence it is called as physical
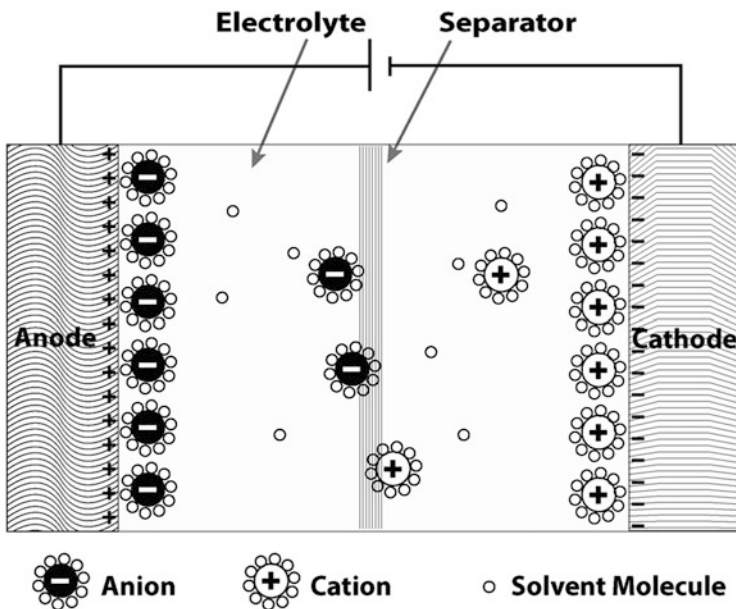
Fig. 3.4 Electric double layer capacitance (EDLC) based supercapacitor is denoted in this image. At the anode the positive charges in the electrode and the hydrated anions in the electrolyte align as a double layer at the electrode–electrolyte interface. On the other hand, the electrons in the cathode and the hydrated cations align as double layer at the electrode–electrolyte interface

charge storage. The double layer thickness at the interface is around 5–10 Å, which strongly depends on the size of the ions being accumulated and the electric field at interface is anticipated to be as high as 10^6 V cm^{-1} (Faraji and Ani 2015). For effective operation of the EDLC supercapacitor the following 5 points have to be satisfied: (a) large surface area (b) better electrical conduction, (c) superior pore size distribution, (d) interconnecting pores, and (e) high wettability (Pandolfo and Hollenkamp 2006).

3.3.2 Pseudocapacitor

Pseudocapacitance is exhibited usually by all non-carbonaceous substances such as conducting polymers and metal oxides. Unlike electric double layer capacitance (EDLC), these materials undergo Faradaic charge-transfer processes resulting in redox reactions (Fig. 3.5). The capacitance in this type is by the swift redox reactions that occur 'near the surface' of the electrode. However, the electrical response of this type of materials is similar to that of EDLC (Pandolfo and Hollenkamp 2006). Pseudocapacitance involves different mechanisms in charge storage such as transition metal oxide based redox reactions, underpotential deposition of 'H' adatoms,
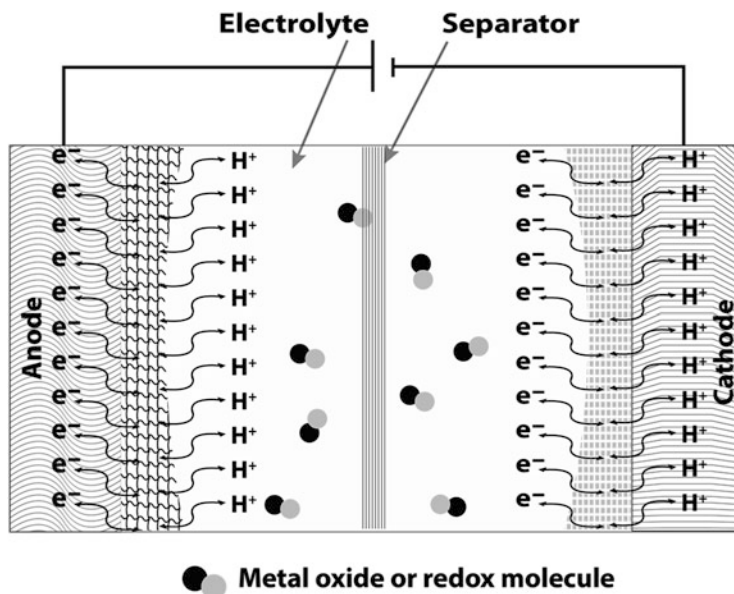
Fig. 3.5 Schematic representation of pseudocapacitance based supercapacitor. Charge crossover at the electrode-electrolyte boundaries occurs through a few layers in the respective electrodes

intercalation reactions in porous materials and doping/de-doping in conducting polymers (Conway and Pell 2003). Comparing the performance based on power burst it is evident that the EDLC type materials have higher power densities compared with that of pseudocapacitance type materials and this is due to the involvement of rate-determining step in Faradaic processes. Moreover, the electrode stability of pseudocapacitance type capacitors are slightly less stable owing to the expansion and contraction of electrode phases during the cycling process and it also leads to poor mechanical stability and retarded cycle life. These types of capacitors display capacitance about 10 to 100 times more than that of EDLC (Chuang et al. 2010).

3.3.3 Hybrid Supercapacitor

The term hybrid supercapacitor was first coined by Amatucci et al. (Amatucci et al. 2001). This group first formed an asymmetric hybrid supercapacitor with activated carbon capacitor electrode as cathode and $Li_4Ti_5O_{12}$ as anode in an organic electrolyte. The idea of forming a hybrid supercapacitor formulated when researchers across the globe looked forward to improve the energy density in a supercapacitor. It is well known that the energy density of supercapacitors range between 5and 10 Wh kg^{-1}. But as the result of hybridization the energy density elevated up to

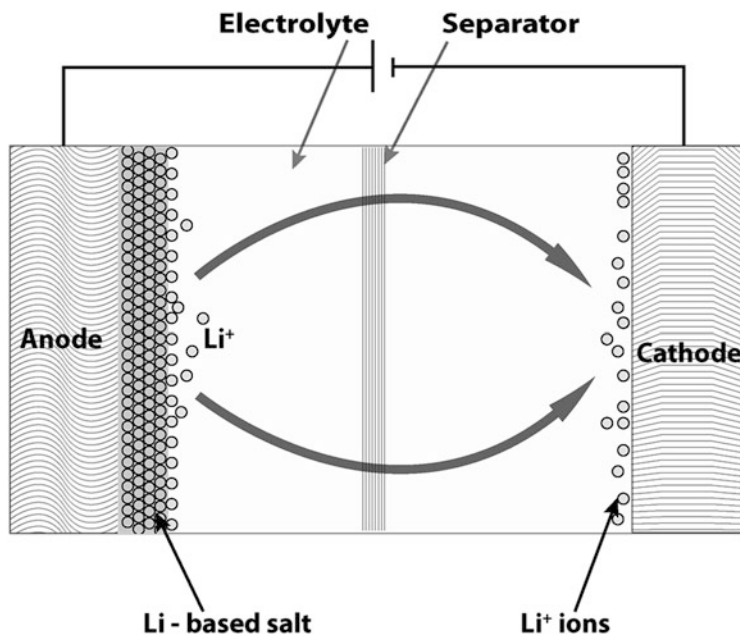**Fig. 3.6** Supercapacitor battery hybrid (SBH) is illustrated in this diagram, battery electrode at the anode has a complete crossover of charge across the electrode–electrolyte interface and the supercapacitor electrode at the cathode has an electrical double layer formation

20 Wh kg^{-1} (Amatucci et al. 2001). Hybrid supercapacitors can be of two major types' viz. external hybrid and internal hybrid. External hybrid is manual connection of readily available supercapacitor to a battery. If they are connected in series, the hybrid would be called external series hybrid or if connected in parallel mode, then the hybrid would be called external parallel hybrid (Cericola and Kötz 2012). If the hybridization of electrodes is made at electrode level it is then called internal hybrid supercapacitor. Even in this case the hybrids could be connected in series or in parallel mode. The scope of this chapter is to deal only with the 'internal hybrid supercapacitor' systems.

The hybrid supercapacitors could also be formed by coupling electric double layer capacitance (EDLC) and pseudocapacitance material in one electrode. This combination provides higher working potential and as a result the capacitance is reported to enhance by two to three times (Wang et al. 2016e). The hybrid capacitors can be either symmetric or asymmetric based on the electrode assembly. Symmetric supercapacitors are assembled through the same type of combined electrodes on both the ends. For instance, combining EDLC and pseudocapacitive components as one hybrid material to be used as both ends of supercapacitor. On the other hand, asymmetric supercapacitors are made of two different electrodes in the following combination, either EDLC and pseudocapacitance electrodes or EDLC and battery type electrodes as shown in Fig. 3.6 (Cericola and Kötz 2012). Hybrid

Table 3.2 Comparison of symmetric, asymmetric and supercapattery hybrid Systems

Parameter	Symmetric Hybrid supercapacitor	Asymmetric hybrid supercapacitor	Supercapacitor battery hybrid (SBH)
Electrode	Same materials	Dissimilar materials	Supercapcitor and Battery type electrode
Energy Density ($W\,h\,kg^{-1}$)	1.13–3.74	5–30	> 30
Power Density ($kW\,kg^{-1}$)	10–20	0.1–5	> 20
Operational Voltage	Individual characteristics of an electrode are observed	Restricts individual characteristics of the electrode	Restricts individual characteristics of the electrode
Example	Co-Al-MWCNTs// Co-Al-MWCNTs	AC//MnO_2	AC//$LiCoO_2$
Charge Storages	Either Non-Faradaic or Faradaic system	Both Faradaic and Non-Faradaic	Both Faradaic and Non-Faradaic

MWCNTs multi-walled carbon nanotubes, *AC* activated carbon

supercapacitors can be either symmetric or asymmetric depending on the exhibition of their supercapacitor behavior. It is to be noted that the symmetric hybrid supercapacitors display better supercapacitive properties than conventional faradaic (pseudocapacitive) or non-faradaic (EDLC) supercapacitors. However, asymmetric supercapacitor-battery hybrids are remarkably efficient than all the other forms of supercapacitors. The comparison on symmetric, asymmetric and a supercapacitor-battery hybrid system are given in Table 3.2. The chapter will briefly discuss each type of the hybrid supercapacitors.

3.3.4 Electrochemical Characteristics of Capacitor, Battery, and Hybrid Systems

The electrochemical characteristics for capacitor, battery, and hybrid systems vary, though the basic construction of all these devices is similar (Conway 2013). The change in the characteristic behavior is graphically represented in Fig. 3.7.

Cyclic voltammetry: The ideal voltammogram of each system has a unique pattern viz. for in a battery, both the electrodes positive and negative, the redox peaks are clearly seen (Fig. 3.7a and b), for in a supercapacitor, it is like a rectangle (Fig. 3.7d and e) and in a hybrid, the voltammogram corresponding to one electrode has redox peaks (Fig. 3.7f) and the other has a rectangle (Fig. 3.7g). In a supercapacitor, the voltage is independent of the current and for a battery the phase changes of a redox reaction are visible. Charge-discharge (CD) curves: the ideal charge-discharge profile for supercapacitor is linear with respect to time (Fig. 3.7f). However, in a battery charge-discharge profile a plateau is observed in
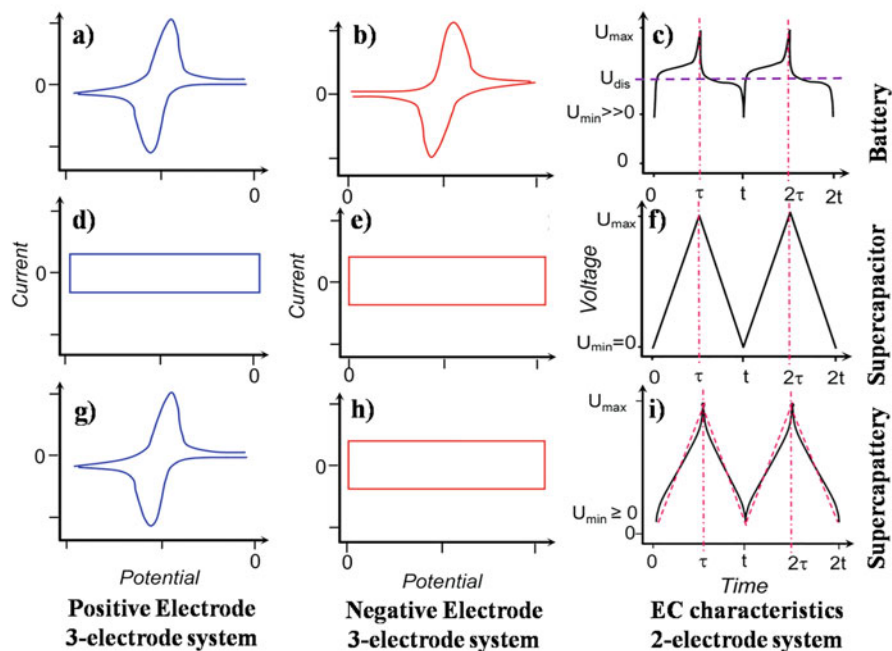
Fig. 3.7 Electrochemical characteristics of **a**, **b** and **c**) battery, **d**, **e** and **f**) supercapacitor and **g**, **h** and **i**) supercapattery systems. Reprinted with permission of Taylor and Francis from (Chen 2017). U_{max} (maximum voltage), U_{min} (minimum voltage), U_{dis} (discharge voltage)

both charging and discharging trend owing to the phase transformation in the redox reactions (Fig. 3.7c). In a hybrid system, the charge-discharge profile is linear with a small curvature in the linearity (Fig. 3.7i). Thus, indicating the incorporation of both the characteristics (Chen 2017).

3.4 Symmetric Hybrid Supercapacitors

In this class of hybrid supercapacitors, both the electrodes are identical in terms of material and composition. However, each electrode is a hybrid in itself. In an investigation, multiwalled carbon nanotubes (MWCNT) were mixed with Co-Al double hydroxides to make it into a composite of active material. Thereafter, the composite material was constructed into two individual electrodes and was assembled as a symmetric hybrid capacitor. Since the process of making a hybrid is related to individual electrodes it is also termed as self-hybrid. The electrolyte used in the process is 1 M KOH. The composite hybridization process largely improved the energy density and power density when compared with normal symmetric supercapacitors with 13.2 Wh kg^{-1} and 6400 W kg^{-1}, respectively (Su et al.

2008). Likewise, all-solid-state symmetric supercapacitors were prepared by Dubal et al. In this work, reduced graphene oxide was coupled with phosphomolybdate (rGO-PMo$_{12}$). A polymer gel electrolyte was used to assemble the system. The energy density displayed by the device was 1.7 mWh cm^{-3} and a maximum power density of 188 mW cm^{-3} was exhibited (Dubal et al. 2015b). In another work, fern-like BiVO$_4$ was made composite with reduced grapheme oxide (rGO) to design the supercapacitor electrode with 6 M KOH as the electrolyte. The system is reported to exhibit volumetric energy density of 1.6 mWh cm^{-3} at 391 mW cm^{-3} (Patil et al. 2016). Purushothaman et al. prepared an active composite of CuO/rGO in a simple low-cost hydrothermal method. This combination is reported to address the issue of poor electrode kinetics with a strategy of combining a transition metal oxide with a carbon-based material. This symmetric hybrid capacitor exhibited energy density of 65.7 Wh kg^{-1} at a power density of 302 W kg^{-1} (Purushothaman et al. 2014). The electrochemical features of the symmetric capacitors are given in Table 3.3.

3.5   Asymmetric Hybrid Supercapacitors

Asymmetric hybrid systems have two different electrodes at both the ends. They may be electric double layer capacitance (EDLC)//pseudocapacitance (vice versa) or pseudocapacitance//pseudocapacitance combinations. But the negative electrode material is different from that of the positive electrode material. These combinations are made to improve the energy and the power density of the system. The pseudocapacitive materials combined with EDLC type materials are expected to contribute with the following features, viz. a) effective faradaic capacitance at the electrode surface providing superior capacitance (surface redox reaction) and b) high power density (above 10^3 W kg^{-1}) along with fast charge-discharge process. Though intercalation may take place at the surface level, they do not behave as batteries (Zuo et al. 2017). They majorly have a CV plot as pseudo-rectangular similar to that of EDLC type materials. Therefore, the combinatorial effect of EDLC and pseudocapacitive materials leaves no big difference in the voltammogram of the hybrid. The combinations of pseudocapacitance//pseudocapacitance also displays voltammogram exhibiting the capacitive behavior.

The prime aim is to improve the energy density of a supercapacitor when an asymmetric supercapacitor is built. However, most of the asymmetric supercapacitor hybrid use carbon type capacitive electrodes as these have electrostatic origin along with high power density, high surface area, superior cycle life and could be used in both aqueous and non-aqueous media (Laforgue et al. 2003). An asymmetric hybrid supercapacitor was assembled with mixed metal Ni, Co hydroxide over reduced grapheme oxide (rGO) as the positive electrode (Ni, Co-OH/rGO) and hierarchical porous carbon as the negative electrode. The system exhibited 37.5 Wh kg^{-1} at 7120 W kg^{-1} with a capacitance retention of about 80% for 17,000 cycles (Ma et al. 2016). In another report, graphene foam and carbon nanotubes (CNTs) were made into composite hybrid film (grapheme foam/CNTs) with high flexibility and perfect

Table 3.3 Symmetric hybrid supercapacitors

Electrode material	Specific capacitance ($F\ g^{-1}$)	Power density ($W\ kg^{-1}$)	Energy density ($Wh\ kg^{-1}$)	Electrolyte	Working voltage (V)	Cycle performance	References
MWCNTs and Co–Al layered double hydroxide	15.2	6400	13.2	1 M KOH	1.6	>1000	Su et al. (2008)
CuO/rGO	326	302	65.7	$0.5MK_2SO_4$	1.2	1500	Purushothaman et al. (2014)
rGO–PMo$_{12}$	$3.18\ F\ cm^{-3}$	$188\ mW\ cm^{-3}$	$1.7\ mW\ h\ cm^{-3}$	PVA/ H$_2$SO$_4$ gel	1.6	5000	Dubal et al. (2015b)
rGO/BiVO$_4$	151	8000	33.7	6 M KOH	1.6	2000	Patil et al. (2016)

MWCNTs multi-walled carbon nanotubes, *rGO* reduced grapheme oxide, *PVA* polyvinyl alcohol

robustness as ideal supporters of holding large quantity of electrochemically active materials. To this support material MnO_2 and polypyrrole (PPy) was individually mixed to form grapheme foam/CNT/MnO_2 and grapheme foam/CNT/PPy, respectively, and were correspondingly made as positive and negative electrodes in an aqueous electrolyte. The system had an output voltage of 1.6 V delivering a 10.3 kW kg^{-1} at 10.9 Wh kg^{-1} (Liu et al. 2014). Capacitance of mixed metal oxide (Co and Ni) nanostructured arrays interconnected with 3D carbon (C/CoNi$_3$O$_4$ NA) over stainless steel to be made as positive electrode for the asymmetric system. The negative electrode of the system was activated carbon. The asymmetric hybrid capacitor exhibited cycling at a high potential of 1.8 V and was efficient upto 19.2 Wh kg^{-1} at a power density of 13 kW kg^{-1} (Zhu et al. 2014).

An asymmetric hybrid supercapacitor was fabricated with NiSe@MoSe$_2$ nanoarrays and nitrogen-doped pamelo mesocarps based carbon nanosheet as positive and negative electrodes, respectively. The interconnection in the sheets of nanoarrays and carbon cause the system to exhibit high specific capacity (128 mAh g^{-1}) and capacitance (223 F g^{-1}). This asymmetric assembly operated at high voltage of 1.6 V displaying an energy density of 0.55 mWh cm^{-3} at 139.1 mW cm^{-3} (Peng et al. 2017). Multidimensional poly (3,4-ethylenedioxythiophene) nanotubes (mPNTs) were prepared by J.E. Lee et al. to investigated the contribution of the morphological features to the electrochemical characteristics of the system. The group built an asymmetric hybrid supercapacitor with MnO_2 loaded mPNTs as the positive electrode and rGO-carbon nanofibers as the negative electrode in an optimized weight ratio of 1:1 leading to superior specific capacitance. The report, however, did not include the energy and power densities (Lee et al. 2014). Yang et al. fabricated a flexible solid-state asymmetric hybrid supercapacitor with α-MnO_2 nanowires and Fe_2O_3 nanotubes grown individually on flexible carbon fabric with a gel electrolyte. The system showed extended response up to 1.6 V and displayed energy density of about 0.55 mWh cm^{-3} at 139.1 mW cm^{-3} (Yang et al. 2014). The electrochemical features of the asymmetric capacitors are given in Table 3.4.

3.6 Supercapacitor—Battery Hybrid (Supercapattery)

Thereafter, the researchers came up with a unique design configuration consisting of a battery electrode and a supercapacitor electrode, termed as supercapacitor—battery hybrid (SBH) or supercapattery hybrid (Fig. 3.6). This is also an asymmetric hybrid system. However, in the previous section, the asymmetric system contained two different electrodes, yet ultimately both the electrodes exhibited supercapacitive behavior only. In the present case of SBH, one electrode exhibits supercapacitive behavior and the other battery type behavior. Notably, though the electrochemical characteristics of both battery and supercapacitor are completely different, the striking similarity between the both is their configurations. Since, both the systems have electrodes such as anode and cathode, electrolyte and a separator. These

Table 3.4 Asymmetric hybrid supercapacitors

Electrode 1 (Positive)	Electrode 2 (Negative)	Specific capacitance (F g^{-1})	Power density (W kg^{-1})	Energy density (Wh kg^{-1})	Electrolyte	Working voltage	Cycle performance	References
Co(OH)$_2$	urchin-like VN	429	15,900	22	2 M KOH	1.6	4000	Wang et al. (2014b)
GF/CNTs/ MnO$_2$	GF/CNTs/PPy	215	860	22.8	0.5 M Na$_2$SO$_4$	1.6	10,000	Liu et al. (2014)
Ni,Co-OH/ rGO	Porous carbon	1691	7120	56.1	6 M KOH	1.6	17,000	Ma et al. (2016)
MnO$_2$– mPNTs^a	rGO–CNFs^a	153	–	–	1 M H$_2$SO$_4$	1.2	1000	Lee et al. (2014)
C/CoNi$_3$O$_4$	Activated carbon	1299	13,000	19.2	3 M KOH	1.8	5000	Zhu et al. (2014)
CF-Co(OH)$_2$	CF-WO$_3$@PPy	2.85	0.12 W cm^{-3}	1.02 mWh cm^{-3}	3 M NaOH	1.6	5000	Wang et al. (2015b)
NiSe@MoSe$_2$	N-PMCN	223	415	32.6	2 M KOH	1.65	5000	Peng et al. (2017)
α-MnO$_2$ nanowires	Fe$_2$O$_3$ nanotubes	–	139.1 mW cm^{-3}	0.55 mWh cm^{-3}	Gel	1.6	6000	Yang et al. (2014)

^{a}*PNTs* poly(3,4-ethylenedioxythiophene), *CNFs* Carbon nanofibers, *N-PMCN* nitrogen-doped pomelo mesocarps-based carbon nanosheet, *GF* graphene foam, *rGO* reduced graphene oxide, *PPy* Polypyrrole

features make the combination or hybridization of two different systems highly feasible. Interesting attribute of this combination is that the direct link between the energy and power components of the system (Zuo et al. 2017). In addition, the system offers ecofriendly trait and safety.

From the previous section we are aware that electric double layer capacitance (EDLC) and pseudocapacitive materials can form a hybrid. Likewise, in this section EDLC (or pseudocapacitive) electrode and battery electrode can form a hybrid. Pseudocapacitive material might be mistakenly understood as a battery material since it also involves 'surface redox reaction'. But the major change is that the battery electrode involves the 'bulk redox reaction'. Here in this hybrid system, the charge separation takes place in a battery electrode, and the electrons flow through the external circuit. The charge separation leads to the movement of anions and cations in the electrolyte. The advantage of this combination over other hybrid systems like symmetric and asymmetric supercapacitive system is that battery component largely improves the energy density and the supercapacitor component largely enhances power density. Notably, each component compensates the other in which the other component is lacking and the final outcome is effectively positive. That is the combinatorial effect is improved in two factors: (i) capacity and (ii) operational voltage (Choi and Park 2014; Khomenko et al. 2008). The capacitance of the SBH is largely improved by about twofold and the operational voltage improves by 1 or 2 V. The battery electrodes involved in the SBHs are Li-ion, Na-ion electrodes, and other ion-based electrodes.

The supercapacitor electrodes utilized could exhibit EDLC or pseudocapacitance properties. So based on these two combinations the following can be derived: a) EDLC—battery hybrids and b) pseudocapacitance—battery hybrid. The battery-supercapacitor system is believed to link two different types of storage mechanisms, the physical and chemical type charge storage. Also, the combinatorial effect of SBHs is expected to be useful in two different ways: a) to possess the excellent features of both a battery and a supercapacitor and b) this combination has the potential to reduce the non-monotonic energy consumption in the batteries (Kouchachvili et al. 2018).

3.6.1 Li-Ion Capacitor

The first ever supercapacitor-battery hybrid (SBH) system was made with Li-ion as the battery component (Amatucci et al. 2001). The combination is also known as Li-ion capacitor or Li-ion hybrid capacitor. Among the materials used for electrochemical storage, it is understood that Li-ion is widely used, in the form of Li-ion batteries and it is extensively employed in portable devices. These capacitors combine the energy storage mechanism of both batteries and supercapacitors. That is, in one of the electrodes, the anions (or cations) adsorb or desorb forming double layer charge storage mechanism. On the other hand, Li-ions are intercalated and deintercalated, where the energy storage follows bulk electrochemical redox

reactions (Wang et al. 2017b). In this system, the Li-ions are reversibly consumed in the charge storage 'rocking chair' process similar to that of in the Li-ion batteries. It is to be noted that the individual electrodes as half cells have to be tested for their charge storage performance before the construction of a whole hybrid system. This is to be done to evaluate the mass loading since one of the electrodes undergoes Faradaic mechanism and the other non-Faradaic mechanism. The mass accumulation balance is one of the prerequisites to be achieved to tap excellent energy density (Mhamane et al. 2016). The total mass loadings are added to calculate the energy density and the power density. The hybrid system is flexible to the usage of both aqueous and non-aqueous electrolytes. However, the advantages of non-aqueous organic electrolyte have been tapped in most of the hybrid systems that include wide voltage window, which largely contributes to better energy density than aqueous electrolyte system.

Amatucci et al. assembled the first SBH with $Li_4Ti_5O_{12}$ as the anode and activated carbon as the cathode. The energy density reported was as high as 20 Wh kg^{-1} in this system (Amatucci et al. 2001). Thereafter, several electrodes were tested for their Li-ion SBH such as, metal oxides TiO_2 (Kim et al. 2013), MnO (Wang et al. 2014a), Nb_2O_5 (Lim et al. 2015), Fe_3O_4 (Zhang et al. 2013), and Si (Liu et al. 2013a), intercalated carbonaceous materials (activated carbon, carbon nanotubes, and graphene) (Wang et al. 2017b) and MnNCN (Liu et al. 2017) as anodes. Moreover, Li metal oxides were used as cathodes viz. $LiMn_2O_4$ (Hu et al. 2009), Li_2CoPO_4F (Karthikeyan et al. 2013), $LiNi_{0.5}Mn_{1.5}O_4$ (Arun et al. 2015), and $Li_3V_2(PO)_4$ (Satish et al. 2015). One of the most commonly used electrodes in this hybrid system is the prelithiated carbon anode, especially of the graphite owing to its low Li-ion intercalation potential and highest cycling stability. Prelithiated carbon electrode can be utilized to harvest energy density of up to 15 Wh kg^{-1} with a cell voltage up to 3.8 V (Zhang et al. 2014a). This system also contributes in preventing the consumption of electrolyte at the anode side and high output voltage. However, the overall specific capacity of the device is lower than that of the batteries and the specific capacitance of the device is higher than the supercapacitors. Activated carbon is another material that plays a pivotal role as electrode in the Li-ion SBH as it is cost effective and has large surface area (Cherusseri et al. 2019). Commercial activated carbon can be utilized as anode and the counter electrode was of mesocarbon microbeads with energy density of 92.3 Wh kg^{-1} and power density of 5.5 kW kg^{-1} (Zhang et al. 2014a). However, a major drawback in this anode is the easy formation of lithium dendrites at the electrode–electrolyte interface. This phenomenon decomposes the electrolyte, poor cycling ability and has safety hazard, thereby preventing a superior performance.

Another section of the EDLC-Li-ion battery hybrid is the use of aqueous electrolytes. The use of aqueous-based electrolytes is deemed superior in terms of safety and ionic conductivity compared with the non-aqueous systems that provide high energy density and extended operational voltage. Aqueous electrolytes are normally nontoxic, nonvolatile, and nonflammable (Luo and Xia 2009). The aqueous salt solutions are neutral viz. Li_2SO_4, LiCl, and $LiNO_3$. The major limitations of the aqueous electrolyte Li-ion SBHs are the poor energy density (< 40 Wh kg^{-1}) and

restrained power density (< 900 W kg^{-1}) (Wang et al. 2006). Apart from these modifications, metal oxides such as $CuBiO_4$ (Yuvaraj et al. 2016), TiO_2, MnO, and Nb_2O_5 also contribute effectively to the Li-ion SBH system. In general, the metal oxide system provides lower $CuBiO_4$ used as negative electrode that has the tendency to exchange its Bi ions for Li-ion through redox reactions or in other words through reversible intercalation. The specific capacitance of this is much lower from the expected value with 26.5 F g^{-1} and low energy density with 24 Wh kg^{-1}. Similarly, TiO_2 along with its composites were examined for negative electrodes in Li-ion capacitors. However, due to their semiconductive nature, they exhibit poor electron conductivity. The limitation can be overcome by reducing the particle size to the nanoscale level, treating with hydrogen and overlaying with a conducting layer. Thereafter, with these changes the TiO_2 produced better results on performance (Kim et al. 2016; Wang et al. 2017b). X. Zhao et al. reported the asymmetric hybrid combination with multi-walled carbon nanotubes (MWCNTs) as the cathode and α-Fe_2O_3/MWCNTs composite as the anode with the Li-ion as the electrolyte. The system exhibited a specific energy density of 50 Wh kg^{-1} and a power density of 1000 W kg^{-1} (Zhao et al. 2009). Metal nitrides also contributed to the formation of Li-ion capacitor and they possess excellent electronic conductivity. NbN has the ability to exhibit power density upto 45 kW kg^{-1} (Wang et al. 2016d). The summary of the electrochemical performances of Li-ion SBH is presented in Table 3.5.

3.6.2   Na-Ion Capacitor

After the successful experimentation with Li-ion electrodes, Na-ion electrodes were tested to form the Na-ion capacitor (or Na-ion supercapacitor battery hybrid [SBH]). The latter was tested for its ability as a battery electrode due to its enormous abundance on the planet earth up to 4–5 orders above Li availability (Wang et al. 2017b). In addition, both Li and Na share common physiochemical properties. The merits of Na in terms of abundance and similar physiochemical property like that of Li make it to be a better choice to replace Li (Yabuuchi et al. 2014). Similar to Li-ion capacitors, in this class of SBHs Na-ion electrodes are mostly used as negative electrodes and the supercapacitive-based materials are used as positive electrodes. Obvious difference between the Li-ion battery electrodes and Na-ion electrodes is that the former has voltammogram as that of a battery, whereas the later is like of capacitive electrode (Ma et al. 2011). One of the main disadvantages of Na in the charge storage device is that it is not compatible with aqueous electrolyte. Therefore, no major work has been reported with Na-ion capacitor using aqueous electrolytes.

In general, the negative electrodes of the Na-ion capacitor includes activated carbon (Kuratani et al. 2012; Wang et al. 2016c), $Na_2Ti_3O_7$ (Yin et al. 2012), $Na_3V_2(PO_4)_3$ (Wang et al. 2015a), Nb_2O_5 (Lim et al. 2016), $NiCo_2O_4$ (Ding et al. 2013), and V_2O_5 (Chen et al. 2012). Likewise, the positive electrodes include, $NaMnO_2$ (Ma et al. 2011), $Na_{0.44}MnO_2$ (Wang et al. 2015d), $Na_x[Fe_{1/2}Mn_{1/2}]O_2$

Table 3.5 Performance of Li-ion capacitors

Supercapacitor electrode	Battery electrode	Specific capacitance ($F\ g^{-1}$)	Power density ($kW\ kg^{-1}$)	Energy density ($Wh\ kg^{-1}$)	Electrolyte	Working voltage (V)	Cycle performance/capacitance retention	References
Activated carbon	$Li_4Ti_5O_{12}$	120	4.3	57	1 M $LiPF_6$ in 1:1 EC[a] and DMC[a]	1–3	2000/92%	Babu et al. (2016)
Activated carbon	$Li-CuBi_2O_4$	26.5	0.3	24	1 M $LiPF_6$ in 1:1:1 EC, DEC[a] and DMC	0–3	1500/86%	Yuvaraj et al. (2016)
Activated carbon	$LiTi_2(PO_4)_3$/Carbon	30	1.0	27	1 M Li_2SO_4	0.3–1.5	1000/85%	Luo and Xia (2009)
Activated carbon	$Li_3V_2(PO_4)_3$/C	–	0.2	27	1 M $LiPF_6$ in 1:1 EC and DMC	3–5	1000/66%	Satish et al. (2015)
Activated carbon	MnO/Carbon	387.7	2.952	227	1 M $LiPF_6$ in 1:1:1 EC, DEC and DMC	0.1–4	5000/76%	Liu et al. (2016)
Graphene	Fe_3O_4/Graphene	–	0.055–4.6	204–65	1 M $LiPF_6$ in 1:1:1 EC, DEC and DMC	0.01–3	1000/70%	Zhang et al. (2013)
Activated carbon	$Li_4Ti_5O_{12}$ (LTO)	165.6	–	20	1 M $LiPF_6$ in 1:1 EC and DMC	1.5–3	5000/85%	Amatucci et al. (2001)
Graphene	Li_3VO_4	206–33	–	110	1 M $LiClO_4$	–	2400/86%	Wang et al. (2017a)
Activated carbon	MnO	30	2.608	220	1 M $LiPF_6$ in 1:1:1 EC, DEC and DMC	0–3.5	3600/95.3	Liu et al. (2017)
N-doped Graphene	$Li_4Ti_5O_{12}$ (LTO)	–	0.2	70	1 M $LiPF_6$ in 1:1:1 EC, DEC and DMC	1–3	10,000/64%	Fan et al. (2016)

Activated 1,2,4,5-benzene tetra carboxylic acid derived carbon	$Li_4Ti_5O_{12}$ (LTO) (	225	0.5 0.5	43.9 63	(1) 1 M $TEA.BF_4$ in ACN (2) 1 M $LiPF_6$ in 1:1 EC and DMC	0–3	6000 / 97%	Mhamane et al. (2016)
Activated carbon	$LiNi_{0.5}Mn_{1.5}O_4$	–		19	1 M $LiPF_6$ in 1:1 EC and DMC	0–3	3000 / 81%	Arun et al. (2015)
Activated carbon	Hydrogen titanate	–	15	33.3	1 M $LiPF_6$ in 1:1 EC and DMC	0–3	3000 / 78.8%	Que et al. (2016)
Graphene	TiO_2/Graphene	205	–	72	Li-ion conducting gel polymer	1–2.5	1000 / 90%	Wang et al. (2015a)
MWCNT	$Li_4Ti_5O_{12}$ (LTO)	109	565 mW/cm^3	4.38 mWh/cm^3	1 M $LiPF_6$ in 1:1 EC and DMC	0–3	3000 / 92%	Zuo et al. (2017)
Activated carbon	Porous NbN	–	45	149	1 M $LiPF_6$ in 1:1 EC and DMC	0–4	15,000 / 95%	Wang et al. (2016d)

[a]*EC* Ethylene carbonate, *DMC* Dimethyl carbonate, *DEC* Diethyl carbonate, *DMC* Dimethyl carbonate, *MWCNT* multi-walled carbon nanotubes, *DMC* Dimethyl carbonate

(Yabuuchi et al. 2012), and $Na_{0.85}Li_{0.17}Ni_{0.21}Mn_{0.64}O_2$ (Kim et al. 2011). In the recent years, the intercalation hard carbon anode and capacitive carbon cathode was studied for the Na-ion SBH. In this case, the intercalated hard carbon displayed poor performance owing to its poor electrochemical behavior in Na-ion based electrolyte. It is to be noted that fast kinetics for Na intercalation in hard carbon and large surface area for capacitive carbon is basically essential for superior performance of the assembled Na-ion capacitor. The condition to improve the working ability of the electrode is to make the electrode highly porous (Kuratani et al. 2012). The required modifications were done in one of the subsequent works where the carbon electrode was constructed using peanut derived activated carbon made as thin flakes and with high porosity. This alteration supported the swift Na-ion intercalation and largely supported the redox reaction. Thereafter, the Na-ion SBH produced energy density of up to 200 Wh kg^{-1} with a power density of up to 16.5 kW kg^{-1} (Ding et al. 2015). The electrochemical performances of Na-ion SBH are presented in Table 3.6.

3.6.3 K-Ion Capacitor

Next element in group 1 of the periodic table that is suitable to be used in supercapacitor battery hybrid (SBH) is K-ion. Notably, like Na, K is also found in abundance across the planet and the redox potential of K (-2.93 V [K$^+$/K] vs standard hydrogen electrode [SHE]) is lower than that of Na (-2.71 V [Na$^+$/Na]).

The atomic size of K does not hinder the gravimetric capacity of the K-ion capacitor. In general, hard carbon is utilized in the K-ion capacitor as the negative electrode. The electrolyte generally used for this section of SBH is 1 M potassium bis (fluorosulfonyl) imide (KFSI) dissolved in ethylene carbonate and diethyl carbonate. Interestingly, ionic conductivity of 1 M KFSI with 10.7 mS cm^{-1} is observed to be superior compared with LiFSI and NaFSI with 9.3 and 9.7 mS cm^{-1}, respectively. This phenomenon largely aids the fast kinetics of metal ion in the electrolyte. However, this capacitor works at a lower working potential, which lies around 0.2 V closer to 0 V and this aids the formation of dendrites at the electrode–electrolyte interface. Moreover, the melting point of potassium (337.15 K) is much lower than that of sodium (371 K) and lithium (453.7 K), which is a safety hazard to the fabricated device.

In order to surmount the demerits displayed by K-ion capacitors several steps have been taken. One of the modifications tested by L. Fan et al. was to replace hard carbon negative electrode with soft carbon. They also replaced the common electrolyte with bis(fluoro-sulfonyl)imide dissolved in dimethyl ether as the electrolyte. This SBH exhibited an energy density of about 120 Wh kg^{-1} and a power density of about 600 W kg^{-1}. The investigation also provided the long desired fast charging and slow discharging behavior (Fan et al. 2018). In another work, the active electrode was replaced with $K_{0.27}MnO_2$ with K_2SO_4 as the electrolyte. This combination has an operational voltage between 0 and 1.9 V displaying an energy density of 25.3 Wh kg^{-1} and power density of 140 W kg^{-1} (Qu et al. 2010). Also, cubic

Table 3.6 Performance of Na-ion capacitors

Supercapacitor electrode	Battery electrode	Power density (kW kg^{-1})	Energy density (Wh kg^{-1})	Electrolyte	Working voltage (V)	Cycle performance / capacitance retention	References
Activated carbon	Spinel NiCo$_2$O$_4$	0.308	13.8	1.5 M NaClO$_4$ PC:DMC^a (1:2)	0–3	2000	Ding et al. (2013)
NaMnO$_2$	Activated carbon	0.13	19.5	0.5 M Na$_2$SO$_4$	0–1.9	10,000	Qu et al. (2009)
Activated carbon	Nb$_2$O$_5$@C/rGO-50	20.8	76	1.0 M NaPF + other	1.0–4.3	3000	Lim et al. (2016)
Carbon mesoporous	Macroporous grapheme	0.501	168	Na$^+$ ion conducting gel	0–4.2	1200	Wang et al. (2015a)
Peanut Shell Hybrid Sodium Ion	Peanut Shell Hybrid Sodium Ion	16.5	201	1 M NaClO$_4$ in 1:1 EC:DEC	1.57–3.5	100,000	Ding et al. (2015)
Activate carbon	V$_2$O$_5$/CNT	45	48	1 M NaClO$_4$ in PC	0–2.8	900	Chen et al. (2012)
Peanut shell carbon	Nb$_2$O$_5$	5.72	43.2	1 M NaClO$_4$ EC: PC (1:1)	1–3	3000/	Li et al. (2016)
Na-ion active carbon	Na$_4$Mn$_9$O$_{18}$	21.0	377.4	1 M Na$_2$SO$_4$ aqueous	0–1.7	4000/	Liu et al. (2013b)
Carbon	Peanut skin derived carbon nanosheets	12	45	1.0 M NaClO$_4$ in 1:1 EC:DEC	0–4	3000	Wang et al. (2016b)
Activated carbon	Porous carbon and NaTiO$_3$ nanotubes	889	34	1.5 M NaClO$_4$ in PC and DMC	0.1–2	1000	Yin et al. (2012)
Na metallic foil	Na$_4$Mn$_9$O$_{18}$	–	–	Polymer Gel	2–4	–	Zhu et al. (2017)

^{a}*EC* Ethylene carbonate, *DEC* Diethyl carbonate, *DEC* Diethyl carbonate, *PC*: Propylene carbonate, *DMC* Dimethyl carbonate, *DEC* diethyl carbonate, *rGO*: Reduced graphene oxide, *CNTs* Carbon nanotubes

Prussian blue crystals ($C_{18}Fe_7N_{18}$) were utilized as the active electrode in K_2SO_4 and this K-ion capacitor showed energy and power densities as 28 Wh kg^{-1} and 214 W kg^{-1}, respectively (Zhou et al. 2017). The summary of the K-ion SBHs electrochemical performances are presented in Table 3.7.

3.6.4 Al-Ion Capacitor

So far, the discussion was on monovalent alkali elements and their role in the supercapacitor battery hybrid (SBH) system. Aluminum is a trivalent ion and the 3-electron transfer during the charge storage offers high efficiency than the monovalent counterparts (Li et al. 2017). Also, Al is highly economical and one of the most abundant metal on the earth's crust. Conductive polypyrrole coated MoO_3 was employed as the negative electrode for the intercalation/deintercalation of Al^{3+} ions in aqueous solution with activated carbon as the positive electrode (Wang et al. 2016a). The energy and power density exhibited by this device was about 28 Wh kg^{-1} and 460 W kg^{-1}, respectively. This system also has ability to exhibit an energy density of 20 Wh kg^{-1} at a power density of 2840 W kg^{-1}. The capacitance of the device was around 693 F g^{-1}, which is thrice than that of the Na-ion capacitor (Wang et al. 2016a). In another work the reversible Al^{3+} ion intercalation in Prussion blue analogs were studied and the energy density of the system was observed to be 13 Wh kg^{-1} (Li et al. 2015). The summary of the Al-ion SBHs electrochemical performances are presented in Table 3.8.

3.6.5 Pseudocapacitor-Battery Hybrid

In general, most of the supercapacitor battery hybrid (SBH) systems employ EDLC type electrodes usually made of carbon. Alternatively, another concept was developed by replacing the double layer capacitive electrodes with pseudocapacitive electrodes. The combination was expected to largely improve the energy density of the SBH devices. It is to be noted that several metal oxides (as discussed here) such as Nb_2O_5 (Lim et al. 2015), MnO_2 and its associates (Ma et al. 2011; Qu et al. 2010; Wang et al. 2015d), MoO_3 (Wang et al. 2016a), TiO_2 (Kim et al. 2013) contribute to the pseudocapacitive behavior. In addition, conducting polymers PANI (polyaniline) and PPy (polypyrrole) also exhibit pseudocapacitive property. However, other electrode materials such as MXenes and MoS_2 are also involved. Advantages of MXenes are that they are two-dimensional (2D) metal carbides that have superior volumetric capacitance compared with all other carbon materials (Zhao et al. 2015b).

Surfaces of MXenes are terminated with O, OH, and F groups and in common they are represented as $M_{n-1}X_nT_x$, where M is the transition metal, X is C or N and T is the terminal groups, and n can be 1, 2 or 3 and x denote the number of terminating

Table 3.7 Performance of K-ion capacitors

Supercapacitor electrode	Battery electrode	Power density (kW kg⁻¹)	Energy density (Wh kg⁻¹)	Electrolyte	Working voltage (V)	Cycle performance / capacitance retention	References
Activated carbon	$K_{0.27}MnO_{2.0}\cdot 6H_2O$	140	25.3	K_2SO_4	0–1.8	10,000 / 98%	Qu et al. (2010)
Graphite	Polyacrylate	–	–	1 M $KN(SO_2F)_2$ in 1:1 EC:DEC	0–3	–	Komaba et al. (2015)
Activated carbon	Prussian Blue	214	28	0.5 M K_2SO_4	1–3	1200 / 98%	Zhou et al. (2017)
Soft carbon	Activated carbon	0.599	120	1 M $KN(SO_2F)_2$ in DME*	1–4	1500 / 97.5%	Fan et al. (2018)

[a]*DME* Dimethoxy ethane, *EC* ethylene carbonate, *DEC* diethyl carbonate

Table 3.8 Performance of Al-ion capacitors

Supercapacitor electrode	Battery electrode	Specific capacitance (F g^{-1})	Power density (kW kg^{-1})	Energy density (Wh kg^{-1})	Electrolyte	Working voltage (V)	Cycle performance / capacitance retention	References
Activated carbon	PPy@MoO$_3$	693	0.46	30	0.5 M Al$_2$(SO$_4$)$_3$	0–1.5	1800 / 93%	Wang et al. (2016a)
Activated carbon	W$_{18}$O$_{49}$ NWs @ SWCNTs	459	0.000295	19	Al^{3+}	0–1.8	5000 / 99.3%	Li et al. (2017)
Activated carbon	Al-0.2 CuFe–PBA	–	–	13	1 M Al (NO$_3$)$_3$	0.2–0.7	1000 /	Li et al. (2015)

SWCNTs single wall carbon nanotubes, *PPy* polypyrrole, *PBA* Prussion blue analogs *NWs* nano-walls.

groups in the given system. These systems can support the intercalation and deintercalation of ions such as Na^+, K^+, NH_4^+, Mg^{2+}, and Al^{3+} provided space for higher capacitance up to 300 F cm^{-3} (Lukatskaya et al. 2013). As understood, the system has more provision for pseudocapacitance. The expected volumetric capacitance of these groups could be up to 450 F cm^{-3} at the scan rate of 2 mV cm^{-2} (Zhao et al. 2015b). MXene Ti_2C employed as a negative electrode with $Na_2Fe_2(SO_4)_3$ as the positive electrode displayed excellent current density. The specific capacitance was several fold above the double layer capacitance (Wang et al. 2015c). Likewise, MoS_2 intercalation and deintercalation with Na-ions are observed to deliver higher capacity to fabricate an effective Na-ion capacitor (Wang et al. 2014c). The electrochemical performances of pseudocapacitor-battery hybrid are presented in Table 3.9.

3.6.6   *Pb-Based Supercapacitor-Battery Hybrid [Acidic]*

Lead acid batteries are safe, economical, and oldest energy storage devices. This system works under the partial state of charge storage, which causes irreversible sulfation of negative electrode leading to its lessened lifespan (Lam et al. 2004). At this juncture, it can be well understood that carbon-based supercapacitors as negative electrode has a superior role to play as they are not easily corroded or evaded (Moseley et al. 2006). This triggered the amalgamation of PbO_2-based battery electrode and activated carbon-based supercapacitor electrodes. PbO_2-based SBHs are the only systems that use highly acidic electrolytes compared with all such similar systems. The system is also known as the lead-carbon capacitors and acidic SBHs. Moreover, this is one of the systems that are successfully commercialized as SBH. The device with PbO_2/activated carbon showed excellent energy density of about 49.4 Wh kg^{-1} and power density of 433.2 W kg^{-1} (Lam et al. 2004). The system could work up to a power density of 2078 W kg^{-1} to render an energy density of 30 Wh kg^{-1}. In another work, PbO_2 thin film and activated carbon was used as the positive and negative electrodes, respectively, in methanesulfonic acid electrolyte. The system exhibited an energy density of about 29 Wh kg^{-1} (Perret et al. 2011). PbO_2 electrodeposited on to graphite was fabricated as SBH along with activated carbon. Operational voltage of this system ranged between 1.88 and 0.65 V. This SBH delivered an energy density of 27 Wh kg^{-1} at a power density of 691 W kg^{-1} (Ni et al. 2013). In another work, PbO_2 thin films were synthesized on Ti/SnO_2 substrates via galvanostatic electrodeposition technique. The device had PbO_2 as the positive electrode and the activated carbon as the negative electrode with H_2SO_4 as the electrolyte. The system displayed energy density of 7.8 Wh kg^{-1} and power density of 258 W kg^{-1} (Yu et al. 2009). Table 3.10 provides the electrochemical performances of acidic SBHs.

Table 3.9 Performance of pseudocapacitor-battery hybrid

Supercapacitor electrode	Battery electrode	Specific capacitance ($F\ g^{-1}$)	Power density ($kW\ kg^{-1}$)	Energy density ($Wh\ kg^{-1}$)	Electrolyte	Working voltage (V)	Cycle performance/ capacitance retention	References
Na foil	MoS_2/G	50	–	–	1 M $NaClO_4$ 1:1 PC: EC 5% FEC*	0.1–2.5	2000 / 81%	Wang et al. (2014c)
Activated carbon	MXene $Ti_3C_2T_x$ / MWCNT	150	–	–	1 M $MgSO_4$	−0.8–0.1	10,000	Zhao et al. (2015a)
Activated carbon	MXene $Ti_3C_2T_x$	81	2.23	3.4	1 M KOH	−0.5–1.0	10,000	Lukatskaya et al. (2013)
$Na_2Fe_2(SO_4)_3$	MXene Ti_2C T_x	245	1.4	260	1 M $NaPF_6$ in 1:1 EC and DEC	0.1–3	100 / 99.7%	Wang et al. (2015c)
Poly aniline derived porous carbon	MoS_2/ Carbon	–	12	111.4	1 M $NaClO_4$ in 1:1:0.05 EC, DEC and FEC	0.4–3	10,000 / 77.3%	Wang et al. (2017c)

[a]*PC* propylene carbonate, *EC* ethylene carbonate, *FEC* fluoroethylene carbonate, *DEC* diethyl carbonate

Table 3.10 Performance of Pb-based supercapacitor-battery hybrids [acidic]

Supercapacitor electrode	Battery electrode	Specific capacitance $(F\,g^{-1})$	Power density $(kW\,kg^{-1})$	Energy density $(Wh\,kg^{-1})$	Electrolyte	Working voltage (V)	Cycle performance/ capacitance retention	References
Activated carbon	PbO_2	34		29	Pb salt in CH_4O_3S	0.7–1.7	3000 / 83%	Perret et al. (2011)
Activated carbon	3D-Ti/ PbO_2	135.2	0.433	49.4	1 M H_2SO_4	1–3	1000 / 99.2%	Zhang et al. (2014b)
Activated carbon	Graphite- PbO_2	63.2	0.152	27	5.3 M H_2SO_4	0.65–1.88	3000 / 80%	Ni et al. (2013)

3.6.7   Ni-Based Supercapacitor Battery Hybrid [Alkaline]

Soon after the invention of Pb acid batteries, the Ni–Cd batteries were also found and unlike the former, the later majorly works in the alkaline electrolytes. In this class, electrospun NiO nanofibers with high aspect ratio and the activated carbon were used as the battery type cathode material and anode material, respectively. The system used 6 M KOH as the electrolyte and had an operating potential of 1.5 V. The setup displayed an energy density of about 43.75 Wh kg^{-1} in a power density of 7500 W kg^{-1} (Kolathodi et al. 2015). In another work, honeycomb-like mesoporous NiO microspheres were used as a cathode material and reduced graphene oxide as anode material. This SBH produced an energy density of 23.25 Wh kg^{-1} and a power density of 9.3 kW kg^{-1} (Ren et al. 2015). Ni(OH)$_2$ is an additional material, which is majorly employed in Ni-based alkaline supercapacitor battery hybrid (SBH) systems.

Hierarchical flower like Ni(OH)$_2$ decorated graphene sheets were coupled with porous graphene as the positive and negative electrodes, respectively. The working voltage of this SBH was noted to be in the region 0–1.6 V with it displaying an energy density of 77.8 Wh kg^{-1} at a power density of 174.7 W kg^{-1} (Yan et al. 2012). Al-substituted α-Ni(OH)$_2$ as positive electrode and activated carbon as the negative electrode was formed as SBH in an alkaline medium. The energy density displayed by the system was 26.9 Wh kg^{-1} at a power density of 1100 W kg^{-1} and it increased upto 42.3 Wh kg^{-1} at 1100 W kg^{-1} (Lang et al. 2010). Furthermore, Ni (OH)$_2$/CNT composite electrode was built on Ni foams to be used as the anode and the activated carbon was employed as the cathode. This combination of SBH displayed an energy density of 50.6 Wh kg^{-1} at a power density of at 95 W kg^{-1} (Tang et al. 2012). Moreover, nanoporous Ni(OH)$_2$ thin film was grown over ultrathin graphite foam (UGF) to be used as positive electrode. Activated microwave exfoliated graphite oxide was used as the negative electrode. An effective power density of 44 kW kg^{-1} was exhibited with an energy density of 13.4 Wh kg^{-1} (Ji et al. 2013).

Additive free NiMoO$_4$ nanosheets or nanorods were synthesized to be used as the positive electrode and activated carbon was used as the negative electrode. The SBH formed had an extended operating voltage of 0–1.7 V with excellent electrochemical performance of 60.9 Wh kg^{-1} energy density at a power density of 850 W kg^{-1} (Peng et al. 2015). Another Ni-based electrode, Ni$_3$S$_2$ loaded onto multi-walled carbon nanotubes was employed as cathode and activated carbon as the anode with 2 M KOH as the electrolyte operating reversibly in the voltage range between 0 and 1.6 V. The system delivered maximum energy density of 19.8 Wh kg^{-1} at 798 W kg^{-1} (Dai et al. 2013). Hierarchical Mn$_{0.4}$Ni$_{0.6}$Co$_2$O$_4$ nanowires were fabricated as positive electrode and activated carbon as the negative electrode with KOH as the electrolyte. The system cycled reversibly at 1.5 V displaying a superior high energy density of 35.2 Wh kg^{-1} (Tamboli et al. 2017). The electrochemical performances displayed by alkaline SBHs are presented in Table 3.11.

Table 3.11 Performance of Ni-based supercapacitor battery hybrid [alkaline]

Supercapacitor electrode	Battery electrode	Specific capacitance (F g^{-1})	Power density (W kg^{-1})	Energy density (Wh kg^{-1})	Electrolyte	Working voltage (V)	Cycle performance/ capacitance retention	References
Activated carbon	Ni(OH)$_2$/ CNT/NF	3300	95	50.6	6 M KOH	1.8	3000 / 87%	Tang et al. (2012)
Porous graphene	Ni(OH)$_2$/ graphene	218.4	174.7	77.8	1 M KOH	1.6	300 / 94.3%	Yan et al. (2012)
Activated carbon	NiMoO$_4$	1221	850	60.9	2 M KOH	1.7	10,000 / 85.7%	Peng et al. (2015)
rGO	NiO microspheres	945	9300	23.25	6 M KOH	1.5	3500 / 88.4%	Ren et al. (2015)
Activated carbon	Ni$_3$S$_2$ and MWCNTs	800	798	19.8	2 M KOH	1.6	5000 / 90%	Dai et al. (2013)
Activated carbon	α-Ni(OH)$_2$	127	1100	46	2 M KOH	1.6	1000 / 82%	Lang et al. (2010)
Activated carbon	Mn$_{1-x}$Ni$_x$Co$_2$O$_4$	1762	–	35.2	2 M KOH	1.5	2000 / 83.2%	Tamboli et al. (2017)
Activated carbon	NiO nanofibers	141	7500	43.75	6 M KOH	1.5	5000 / 88%	Kolathodi et al. (2015)
Activated carbon	Graphene– nickel cobaltite	618	5600	19.5	6 M KOH	1.4	10,000 / 102%	Wang et al. (2012)
a-MEGO[a]	Ni(OH)$_2$/ UGF[a]	166	44,000	13.4	6 M KOH	1.8	10,000 / 63.2%	Ji et al. (2013)

[a]*a-MEGO* activated microwave exfoliated graphite oxide, *UGF* Ultrathin graphene foam, *CNTs* carbon nanotubes, *MWCNTs* multi-wall carbon nanotubes, *NF* Nickel Foam

3.6.8 Effectiveness of Supercapattery Systems

The hybridization of a capacitor and a battery into a single system has innate advantages and it could be explained with the charging potential profiles as illustrated in Fig. 3.8. The primary change witnessed is in the voltage limit expansion: the charging potential for a supercapacitor (Fig. 3.8a) is linear with respect to time in a given voltage limits (ΔV_c). Likewise, the charging potential of the battery system (Fig. 3.8b) is in parabolic form, which includes a redox phase change in a given voltage limit (ΔV_b). In a supercapacitor battery hybrid (SBH) system, a combinatorial effect (Fig. 3.8c) takes place with an increase in the voltage limits (ΔV) with the final equation (Dubal et al. 2015a) being,

$$\Delta V = \Delta V_c + \Delta V_b \tag{3.6}$$

Thus, the increase in voltage is obvious. Thereafter, the SBH exhibits an expansion in the energy storage: the supercapacitors render high power density and the battery render high energy density. The amalgamation of two such components in SBHs improves the energy storage with a contribution from both (Chen 2017). Energy stored in a battery and supercapacitor is given as below, respectively,

$$E_b = Q_b . \Delta V_b \tag{3.7}$$

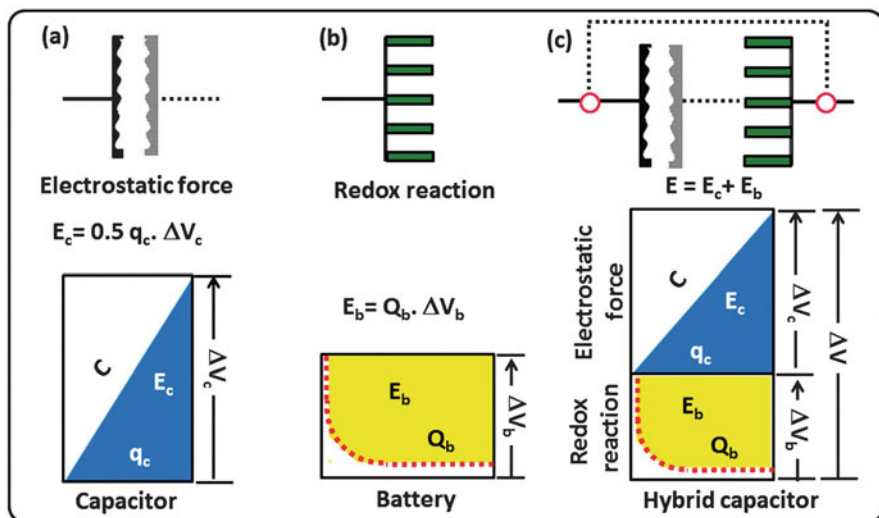**Fig. 3.8** Electrode systems (**a**) capacitor (**b**) battery, and (**c**) an asymmetric supercapacitor-battery hybrid. (Reprinted with permission of RSC from Dubal et al. 2015a)

$$E_c = 0.5q_c.\Delta V_c \tag{3.8}$$

where E_b and E_c are energy stored in battery and supercapacitor, respectively. Q_b and q_c are the charges stored in battery and supercapacitor, respectively. It is to be noted that the energy stored in a capacitor is half than that of the battery. The total energy stored (Fig. 3.8c) in a SBH system (Dubal et al. 2015a) is given as,

$$E_{SBH} = E_b + E_c \tag{3.9}$$

Apart from these fundamental changes, the supercapacitor and battery components compensate the each other with the lacking energy density and power density, respectively.

3.7 Conclusion

This chapter provides an outline to understand the improvements in the supercapacitor sector. The hybrid supercapacitor systems are in the line of current electrochemical energy storage systems. Earlier, it was development only in the EDLC or pseudocapacitance systems. Now, it is a combination of both and the addition of battery electrodes in supercapacitor devices. The supercapacitor-battery hybrid has brought in excellent energy density rendering devices at a superior power density and is still prone to advancement. The field is swiftly expanding and advanced outputs are anticipated.

References

Amatucci GG, Badway F, Du Pasquier A, Zheng T (2001) An asymmetric hybrid nonaqueous energy storage cell. J Electrochem Soc 148:A930–A939. https://doi.org/10.1149/1.1383553

Arun N, Jain A, Aravindan V, Jayaraman S, Ling WC, Srinivasan MP, Madhavi S (2015) Nanostructured spinel $LiNi_{0.5}Mn_{1.5}O_4$ as new insertion anode for advanced Li-ion capacitors with high power capability. Nano Energ 12:69–75. https://doi.org/10.1016/j.nanoen.2014.12.006

Babu B, Lashmi P, Shaijumon M (2016) Li-ion capacitor based on activated rice husk derived porous carbon with improved electrochemical performance. Electrochim Acta 211:289–296. https://doi.org/10.1016/j.electacta.2016.06.055

Cericola D, Kötz R (2012) Hybridization of rechargeable batteries and electrochemical capacitors: principles and limits. Electrochim Acta 72:1–17. https://doi.org/10.1016/j.electacta.2012.03.151

Chen GZ (2017) Supercapacitor and supercapattery as emerging electrochemical energy stores. Int Mater Rev 62:173–202. https://doi.org/10.1080/09506608.2016.1240914

Chen PC, Shen G, Shi Y, Chen H, Zhou C (2010) Preparation and characterization of flexible asymmetric supercapacitors based on transition-metal-oxide nanowire/single-walled carbon nanotube hybrid thin-film electrodes. ACS Nano 4:4403–4411. https://doi.org/10.1021/nn100856y

Chen Z, Augustyn V, Jia X, Xiao Q, Dunn B, Lu Y (2012) High-performance sodium-ion pseudocapacitors based on hierarchically porous nanowire composites. ACS Nano 6:4319–4327. https://doi.org/10.1021/nn300920e

Cherusseri J, Kumar KS, Choudhary N, Nagaiah N, Jung Y, Roy T, Thomas J (2019) Novel mesoporous electrode materials for symmetric, asymmetric and hybrid supercapacitors. Nanotechnol 30:202001. https://doi.org/10.1088/1361-6528/ab0685

Choi HS, Park CR (2014) Theoretical guidelines to designing high performance energy storage device based on hybridization of lithium-ion battery and supercapacitor. J Power Sources 259:1–14. https://doi.org/10.1016/j.jpowsour.2014.02.001

Chuang CM, Huang CW, Teng H, Ting JM (2010) Effects of carbon nanotube grafting on the performance of electric double layer capacitors. Energ Fuel 24:6476–6482. https://doi.org/10.1021/ef101208x

Conway BE (2013) Electrochemical supercapacitors: scientific fundamentals and technological applications. Springer. https://doi.org/10.1007/978-1-4757-3058-6

Conway B, Pell W (2003) Double-layer and pseudocapacitance types of electrochemical capacitors and their applications to the development of hybrid devices. J Solid State Electrochem 7:637–644. https://doi.org/10.1007/s10008-003-0395-7

Dai C-S et al (2013) Hierarchically structured Ni_3S_2/carbon nanotube composites as high performance cathode materials for asymmetric supercapacitors. ACS Appl Mater Interfaces 5:12168–12174. https://doi.org/10.1021/am404196s

Ding R, Qi L, Wang H (2013) An investigation of spinel $NiCo_2O_4$ as anode for Na-ion capacitors. Electrochim Acta 114:726–735. https://doi.org/10.1016/j.electacta.2013.10.113

Ding J et al (2015) Peanut shell hybrid sodium ion capacitor with extreme energy–power rivals lithium ion capacitors. Energy Environ Sci 8:941–955. https://doi.org/10.1039/C4EE02986K

Du X et al (2013) Preparation of activated carbon hollow fibers from ramie at low temperature for electric double-layer capacitor applications. Bioresour Technol 149:31–37. https://doi.org/10.1016/j.biortech.2013.09.026

Dubal DP, Ayyad O, Ruiz V, Gomez-Romero P (2015a) Hybrid energy storage: the merging of battery and supercapacitor chemistries. Chem Soc Rev 44:1777–1790. https://doi.org/10.1039/C4CS00266K

Dubal DP, Suarez-Guevara J, Tonti D, Enciso E, Gomez-Romero P (2015b) A high voltage solid state symmetric supercapacitor based on graphene–polyoxometalate hybrid electrodes with a hydroquinone doped hybrid gel-electrolyte. J Mater Chem A 3:23483–23492. https://doi.org/10.1039/c5ta05660h

Endo M, Takeda T, Kim Y, Koshiba K, Ishii K (2001) High power electric double layer capacitor (EDLC's); from operating principle to pore size control in advanced activated carbons. Carbon lett 1:117–128

Fan Q, Yang M, Meng Q, Cao B, Yu Y (2016) Activated-nitrogen-doped graphene-based aerogel composites as cathode materials for high energy density lithium-ion supercapacitor. J Electrochem Soc 163:A1736–A1742. https://doi.org/10.1149/2.1271608jes

Fan L, Lin K, Wang J, Ma R, Lu B (2018) A nonaqueous potassium-based battery–Supercapacitor hybrid device. Adv Mater 30:1800804. https://doi.org/10.1002/adma.201800804

Faraji S, Ani FN (2015) The development supercapacitor from activated carbon by electroless plating—a review. Renew Sust Energ Rev 42:823–834. https://doi.org/10.1016/j.rser.2014.10.068

Fernández J, Morishita T, Toyoda M, Inagaki M, Stoeckli F, Centeno TA (2008) Performance of mesoporous carbons derived from poly (vinyl alcohol) in electrochemical capacitors. J Power Sources 175:675–679. https://doi.org/10.1016/j.jpowsour.2007.09.042

González A, Goikolea E, Barrena JA, Mysyk R (2016) Review on supercapacitors: technologies and materials. Renew Sust Energ Rev 58:1189–1206. https://doi.org/10.1016/j.rser.2015.12.249

Hu X, Deng Z, Suo J, Pan Z (2009) A high rate, high capacity and long life ($LiMn_2O_4$+ AC)/$Li_4Ti_5O_{12}$ hybrid battery–supercapacitor. J Power Sources 187:635–639. https://doi.org/10.1016/j.jpowsour.2008.11.033

Ji J et al (2013) Nanoporous $Ni(OH)_2$ thin film on 3D ultrathin-graphite foam for asymmetric supercapacitor. ACS Nano 7:6237–6243. https://doi.org/10.1021/nn4021955

Jorio A et al (2001) Structural (n, m) determination of isolated single-wall carbon nanotubes by resonant Raman scattering. Phys Rev Lett 86:1118. https://doi.org/10.1103/PhysRevLett.86.1118

Karthikeyan K, Amaresh S, Kim K, Kim S, Chung K, Cho B, Lee Y (2013) A high performance hybrid capacitor with Li_2CoPO_4F cathode and activated carbon anode. Nanoscale 5:5958–5964. https://doi.org/10.1039/C3NR00760J

Khomenko V, Raymundo-Piñero E, Béguin F (2008) High-energy density graphite/AC capacitor in organic electrolyte. J Power Sources 177:643–651. https://doi.org/10.1016/j.jpowsour.2007.11.101

Kim D et al (2011) Enabling sodium batteries using lithium-substituted sodium layered transition metal oxide cathodes. Adv Energ Mater 1:333–336. https://doi.org/10.1002/aenm.201000061

Kim H et al (2013) A novel high-energy hybrid supercapacitor with an anatase TiO_2–reduced graphene oxide anode and an activated carbon cathode. Adv Energ Mater 3:1500–1506. https://doi.org/10.1002/aenm.201300467

Kim H-K et al (2016) TiO_2-reduced graphene oxide nanocomposites by microwave-assisted forced hydrolysis as excellent insertion anode for Li-ion battery and capacitor. J Power Sources 327:171–177. https://doi.org/10.1016/j.jpowsour.2016.07.053

Kolathodi MS, Palei M, Natarajan TS (2015) Electrospun NiO nanofibers as cathode materials for high performance asymmetric supercapacitors. J Mater Chem A 3:7513–7522. https://doi.org/10.1039/C4TA07075E

Komaba S, Hasegawa T, Dahbi M, Kubota K (2015) Potassium intercalation into graphite to realize high-voltage/high-power potassium-ion batteries and potassium-ion capacitors. Electrochem Commun 60:172–175. https://doi.org/10.1016/j.elecom.2015.09.002

Kouchachvili L, Yaïci W, Entchev E (2018) Hybrid battery/supercapacitor energy storage system for the electric vehicles. J Power Sources 374:237–248. https://doi.org/10.1016/j.jpowsour.2017.11.040

Kuratani K, Yao M, Senoh H, Takeichi N, Sakai T, Kiyobayashi T (2012) Na-ion capacitor using sodium pre-doped hard carbon and activated carbon. Electrochim Acta 76:320–325. https://doi.org/10.1016/j.electacta.2012.05.040

Laforgue A et al (2003) Activated carbon/conducting polymer hybrid supercapacitors. J Electrochem Soc 150:A645–A651. https://doi.org/10.1149/1.1566411

Lam L, Haigh N, Phyland C, Urban A (2004) Failure mode of valve-regulated lead-acid batteries under high-rate partial-state-of-charge operation. J Power Sources 133:126–134. https://doi.org/10.1016/j.jpowsour.2003.11.048

Lang J-W, Kong L-B, Liu M, Luo Y-C, Kang L (2010) Asymmetric supercapacitors based on stabilized α-$Ni(OH)_2$ and activated carbon. J Solid State Electr 14:1533–1539. https://doi.org/10.1007/s10008-009-0984-1

Lee SW, Gallant BM, Byon HR, Hammond PT, Shao-Horn Y (2011) Nanostructured carbon-based electrodes: bridging the gap between thin-film lithium-ion batteries and electrochemical capacitors. Energy Environ Sci 4:1972–1985. https://doi.org/10.1039/C0EE00642D

Lee JE, Park SJ, Kwon OS, Shim HW, Jang J, Yoon H (2014) Systematic investigation on charge storage behaviour of multidimensional poly(3, 4-ethylenedioxythiophene)nanostructures. RSC Adv 4:37529–37535. https://doi.org/10.1039/C4RA06161F

Li Z, Xiang K, Xing W, Carter WC, Chiang Y-M (2015) Reversible aluminum-ion intercalation in prussian blue analogs and demonstration of a high-power aluminum-ion asymmetric capacitor. Adv Energ Mater 5:1401410. https://doi.org/10.1002/aenm.201401410

Li H, Zhu Y, Dong S, Shen L, Chen Z, Zhang X, Yu G (2016) Self-assembled Nb_2O_5 nanosheets for high energy–high power sodium ion capacitors. Chem Mater 28:5753–5760. https://doi.org/10.1021/acs.chemmater.6b01988

Li K, Shao Y, Liu S, Zhang Q, Wang H, Li Y, Kaner RB (2017) Aluminum-ion-intercalation supercapacitors with ultrahigh areal capacitance and highly enhanced cycling stability: power supply for flexible Electrochromic devices. Small 13:1700380. https://doi.org/10.1002/smll.201700380

Lim E et al (2015) Facile synthesis of Nb2O5@ carbon core–shell nanocrystals with controlled crystalline structure for high-power anodes in hybrid supercapacitors. ACS Nano 9:7497–7505. https://doi.org/10.1021/acsnano.5b02601

Lim E et al (2016) High-performance sodium-ion hybrid supercapacitor based on Nb_2O_5@ carbon core–shell nanoparticles and reduced graphene oxide nanocomposites. Adv Funct Mater 26:3711–3719. https://doi.org/10.1002/adfm.201505548

Liu X, Jung H-G, Kim S-O, Choi H-S, Lee S, Moon JH, Lee JK (2013a) Silicon/copper dome-patterned electrodes for high-performance hybrid supercapacitors. Sci Rep 3:3183. https://doi.org/10.1038/srep03183

Liu X, Zhang N, Ni J, Gao L (2013b) Improved electrochemical performance of sol–gel method prepared $Na_4Mn_9O_{18}$ in aqueous hybrid Na-ion supercapacitor. J Sol State Electrochem 17:1939–1944. https://doi.org/10.1007/s10008-013-2044-0

Liu J, Zhang L, Wu HB, Lin J, Shen Z, Lou XWD (2014) High-performance flexible asymmetric supercapacitors based on a new graphene foam/carbon nanotube hybrid film. Energy Environ Sci 7:3709–3719. https://doi.org/10.1039/C4EE01475H

Liu C, Zhang C, Song H, Zhang C, Liu Y, Nan X, Cao G (2016) Mesocrystal MnO cubes as anode for Li-ion capacitors. Nano Energ 22:290–300. https://doi.org/10.1016/j.nanoen.2016.02.035

Liu C, Zhang C, Fu H, Nan X, Cao G (2017) Exploiting high-performance anode through tuning the character of chemical bonds for Li-ion batteries and capacitors. Adv Energ Mater 7:1601127. https://doi.org/10.1002/aenm.201601127

Lu Z, Chang Z, Zhu W, Sun X (2011) Beta-phased $Ni(OH)_2$ nanowall film with reversible capacitance higher than theoretical faradic capacitance. Chem Commun 47:9651–9653. https://doi.org/10.1039/C1CC13796D

Lukatskaya MR et al (2013) Cation intercalation and high volumetric capacitance of two-dimensional titanium carbide. Science 341:1502–1505. https://doi.org/10.1126/science.1241488

Luo J-Y, Xia Y-Y (2009) Electrochemical profile of an asymmetric supercapacitor using carbon-coated $LiTi_2(PO_4)_3$ and active carbon electrodes. J Power Sources 186:224–227. https://doi.org/10.1016/j.jpowsour.2008.09.063

Ma X, Chen H, Ceder G (2011) Electrochemical properties of monoclinic $NaMnO_2$. J Electrochem Soc 158:A1307–A1312. https://doi.org/10.1149/2.035112jes

Ma H, He J, Xiong D-B, Wu J, Li Q, Dravid V, Zhao Y (2016) Nickel cobalt hydroxide@reduced graphene oxide hybrid nanolayers for high performance asymmetric supercapacitors with remarkable cycling stability. ACS Appl Mater Interfaces 8:1992–2000. https://doi.org/10.1021/acsami.5b10280

Mhamane D et al (2016) Silica-assisted bottom-up synthesis of graphene-like high surface area carbon for highly efficient ultracapacitor and Li-ion hybrid capacitor applications. J Mater Chem A 4:5578–5591. https://doi.org/10.1039/C6TA00868B

Moseley P, Nelson R, Hollenkamp A (2006) The role of carbon in valve-regulated lead–acid battery technology. J Power Sources 157:3–10. https://doi.org/10.1016/j.jpowsour.2006.02.031

Muzaffar A, Ahamed MB, Deshmukh K, Thirumalai J (2019) A review on recent advances in hybrid supercapacitors: design, fabrication and applications. Renew Sust Energ Rev 101:123–145. https://doi.org/10.1016/j.rser.2018.10.026

Ni J, Wang H, Qu Y, Gao L (2013) PbO_2 electrodeposited on graphite for hybrid supercapacitor applications. Phys Scr 87:045802. https://doi.org/10.1088/0031-8949/87/04/045802

Pandolfo A, Hollenkamp A (2006) Carbon properties and their role in supercapacitors. J Power Sources 157:11–27. https://doi.org/10.1016/j.jpowsour.2006.02.065

Patil SS et al (2016) Fern-like $rGO/BiVO_4$ hybrid nanostructures for high-energy symmetric supercapacitor. ACS Appl Mater Interfaces 8:31602–31610. https://doi.org/10.1021/acsami.6b08165

Peng S, Li L, Wu HB, Madhavi S, Lou XW (2015) Controlled growth of $NiMoO_4$ nanosheet and nanorod arrays on various conductive substrates as advanced electrodes for asymmetric supercapacitors. Adv Energ Mater 5:1401172. https://doi.org/10.1002/aenm.201401172

Peng H, Zhou J, Sun K, Ma G, Zhang Z, Feng E, Lei Z (2017) High-performance asymmetric supercapacitor designed with a novel NiSe@ $MoSe_2$ nanosheet array and nitrogen-doped carbon nanosheet. ACS Sust Chem Engg 5:5951–5963. https://doi.org/10.1021/acssuschemeng.7b00729

Perret P, Khani Z, Brousse T, Bélanger D, Guay D (2011) Carbon/PbO_2 asymmetric electrochemical capacitor based on methanesulfonic acid electrolyte. Electrochim Acta 56:8122–8128. https://doi.org/10.1016/j.electacta.2011.05.125

Plitz I, DuPasquier A, Badway F, Gural J, Pereira N, Gmitter A, Amatucci G (2006) The design of alternative nonaqueous high power chemistries. Appl Phys A Mater Sci Process 82:615–626. https://doi.org/10.1007/s00339-005-3420-0

Purushothaman KK, Saravanakumar B, Babu IM, Sethuraman B, Muralidharan G (2014) Nano-structured CuO/reduced graphene oxide composite for hybrid supercapacitors. RSC Adv 4:23485–23491. https://doi.org/10.1039/C4RA02107J

Qu D, Shi H (1998) Studies of activated carbons used in double-layer capacitors. J Power Sources 74:99–107. https://doi.org/10.1016/S0378-7753(98)00038-X

Qu Q, Shi Y, Tian S, Chen Y, Wu Y, Holze R (2009) A new cheap asymmetric aqueous supercapacitor: activated carbon//$NaMnO_2$. J Power Sources 194:1222–1225. https://doi.org/10.1016/j.jpowsour.2009.06.068

Qu Q, Li L, Tian S, Guo W, Wu Y, Holze R (2010) A cheap asymmetric supercapacitor with high energy at high power: activated carbon//$K_{0.27}MnO_2 \cdot 0.6H_2O$. J Power Sources 195:2789–2794. https://doi.org/10.1016/j.jpowsour.2009.10.108

Que L, Wang Z, Yu F, Gu D (2016) 3D ultralong nanowire arrays with a tailored hydrogen titanate phase as binder-free anodes for Li-ion capacitors. J Mater Chem A 4:8716–8723. https://doi.org/10.1039/C6TA02413K

Ren X, Guo C, Xu L, Li T, Hou L, Wei Y (2015) Facile synthesis of hierarchical mesoporous honeycomb-like NiO for aqueous asymmetric supercapacitors. ACS Appl Mater Interfaces 7:19930–19940. https://doi.org/10.1021/acsami.5b04094

Satish R, Aravindan V, Ling WC, Madhavi S (2015) Carbon-coated $Li_3V_2(PO_4)_3$ as insertion type electrode for lithium-ion hybrid electrochemical capacitors: an evaluation of anode and cathodic performance. J Power Sources 281:310–317. https://doi.org/10.1016/j.jpowsour.2015.01.190

Sharma P, Bhatti T (2010) A review on electrochemical double-layer capacitors. Energ Convers Manage 51:2901–2912. https://doi.org/10.1016/j.enconman.2010.06.031

Su L, Zhang X, Yuan C, Gao B (2008) Symmetric self-hybrid supercapacitor consisting of multiwall carbon nanotubes and Co–Al layered double hydroxides. J Electrochem Soc 155:A110–A114. https://doi.org/10.1149/1.2806844

Tamboli MS et al (2017) Mimics of microstructures of Ni substituted $Mn_{1-x}Ni_xCo_2O_4$ for high energy density asymmetric capacitors. Chem Engg J 307:300–310. https://doi.org/10.1016/j.cej.2016.08.086

Tang Z, Tang C-h, Gong H (2012) A high energy density asymmetric supercapacitor from nano-architectured Ni(OH)$_2$/Carbon nanotube electrodes. Adv Funct Mater 22:1272–1278. https://doi.org/10.1002/adfm.201102796

Wang Y-G, Luo J-Y, Wang C-X, Xia Y-Y (2006) Hybrid Aqueous Energy Storage Cells Using Activated Carbon and Lithium-Ion Intercalated Compounds II. Comparison of LiMn$_2$O$_4$, LiCo$_{1/3}$Ni$_{1/3}$Mn$_{1/3}$O$_2$, and LiCoO$_2$ Positive Electrodes. J Electrochem Soc 153:A1425–A1431

Wang H et al (2012) Graphene-nickel cobaltite nanocomposite asymmetrical supercapacitor with commercial level mass loading. Nano Res 5:605–617. https://doi.org/10.1007/s12274-012-0246-x

Wang H et al (2014a) Hybrid device employing three-dimensional arrays of MnO in carbon nanosheets bridges battery–supercapacitor divide. Nano Lett 14:1987–1994. https://doi.org/10.1021/nl500011d

Wang R, Yan X, Lang J, Zheng Z, Zhang P (2014b) A hybrid supercapacitor based on flower-like Co(OH)$_2$ and urchin-like VN electrode materials. J Mater Chem A 2:12724–12732. https://doi.org/10.1039/C4TA01296H

Wang Y-X, Chou S-L, Wexler D, Liu H-K, Dou S-X (2014c) High-performance sodium-ion batteries and sodium-ion Pseudocapacitors based on MoS$_2$/graphene composites. Chem Eur J 20:9607–9612. https://doi.org/10.1002/chem.201402563

Wang F et al (2015a) A quasi-solid-state sodium-ion capacitor with high energy density. Adv Mater 27:6962–6968. https://doi.org/10.1002/adma.201503097

Wang F et al (2015b) Tungsten oxide@polypyrrole core–shell nanowire arrays as novel negative electrodes for asymmetric supercapacitors. Small 11:749–755. https://doi.org/10.1002/smll.201402340

Wang X et al (2015c) Pseudocapacitance of MXene nanosheets for high-power sodium-ion hybrid capacitors. Nat Commun 6:6544. https://doi.org/10.1038/ncomms7544

Wang Y et al (2015d) Ti-substituted tunnel-type Na$_{0.44}$MnO$_2$ oxide as a negative electrode for aqueous sodium-ion batteries. Nat Commun 6:6401. https://doi.org/10.1038/ncomms7401

Wang F et al (2016a) A conductive polymer coated MoO$_3$ anode enables an Al-ion capacitor with high performance. J Mater Chem A 4:5115–5123. https://doi.org/10.1039/C6TA01398H

Wang H, Mitlin D, Ding J, Li Z, Cui K (2016b) Excellent energy–power characteristics from a hybrid sodium ion capacitor based on identical carbon nanosheets in both electrodes. J Mater Chem A 4:5149–5158. https://doi.org/10.1039/C6TA01392A

Wang H, Mitlin D, Ding J, Li Z, Cui K (2016c) Excellent energy–power characteristics from a hybrid sodium ion capacitor based on identical carbon nanosheets in both electrodes. J Mater Chem A 4:5149–5158. https://doi.org/10.1039/C6TA01392A

Wang P, Wang R, Lang J, Zhang X, Chen Z, Yan X (2016d) Porous niobium nitride as a capacitive anode material for advanced Li-ion hybrid capacitors with superior cycling stability. J Mater Chem A 4:9760–9766. https://doi.org/10.1039/C6TA02971J

Wang Q, Nie YF, Chen XY, Xiao ZH, Zhang ZJ (2016e) Controllable synthesis of 2D amorphous carbon and partially graphitic carbon materials: large improvement of electrochemical performance by the redox additive of sulfanilic acid azochromotrop in KOH electrolyte. Electrochim Acta 200:247–258. https://doi.org/10.1016/j.electacta.2016.03.183

Wang F et al (2017a) A quasi-solid-state Li-ion capacitor with high energy density based on Li$_3$VO$_4$/carbon nanofibers and electrochemically-exfoliated graphene sheets. J Mater Chem A 5:14922–14929. https://doi.org/10.1039/C7TA03920D

Wang F et al (2017b) Latest advances in supercapacitors: from new electrode materials to novel device designs. Chem Soc Rev 46:6816–6854. https://doi.org/10.1039/C7CS00205J

Wang R, Wang S, Peng X, Zhang Y, Jin D, Chu PK, Zhang L (2017c) Elucidating the intercalation pseudocapacitance mechanism of MoS$_2$–carbon monolayer interoverlapped superstructure: toward high-performance sodium-ion-based hybrid supercapacitor. ACS Appl Mater Interfaces 9:32745–32755. https://doi.org/10.1021/acsami.7b09813

Winter M, Brodd RJ (2004) What are batteries, fuel cells, and supercapacitors? Chem Rev 104:4245–4269. https://doi.org/10.1021/cr020730k

Yabuuchi N et al (2012) P2-type $Na_x[Fe_{1/2}Mn_{1/2}]O_2$ made from earth-abundant elements for rechargeable Na batteries. Nat Mater 11:512. https://doi.org/10.1038/nmat3309

Yabuuchi N, Kubota K, Dahbi M, Komaba S (2014) Research development on sodium-ion batteries. Chem Rev 114:11636–11682. https://doi.org/10.1021/cr500192f

Yan J et al (2012) Advanced asymmetric supercapacitors based on $Ni(OH)_2$/graphene and porous graphene electrodes with high energy density. Adv Funct Mater 22:2632–2641. https://doi.org/10.1002/adfm.201102839

Yang P et al (2014) Low-cost high-performance solid-state asymmetric supercapacitors based on MnO_2 nanowires and Fe_2O_3 nanotubes. Nano Lett 14:731–736. https://doi.org/10.1021/nl404008e

Yin J, Qi L, Wang H (2012) Sodium titanate nanotubes as negative electrode materials for sodium-ion capacitors. ACS Appl Mater Interface 4:2762–2768. https://doi.org/10.1021/am300385r

Yu N, Gao L, Zhao S, Wang Z (2009) Electrodeposited PbO_2 thin film as positive electrode in PbO_2/AC hybrid capacitor. Electrochim Acta 54:3835–3841. https://doi.org/10.1016/j.electacta.2009.01.086

Yuvaraj S, Karthikeyan K, Kalpana D, Lee YS, Selvan RK (2016) Surfactant-free hydrothermal synthesis of hierarchically structured spherical $CuBi_2O_4$ as negative electrodes for Li-ion hybrid capacitors. J Colloid Interface Sci 469:47–56. https://doi.org/10.1016/j.jcis.2016.01.060

Zhang LL, Zhao X (2009) Carbon-based materials as supercapacitor electrodes. Chem Soc Rev 38:2520–2531. https://doi.org/10.1039/B813846J

Zhang F, Zhang T, Yang X, Zhang L, Leng H, Huang Y, Chen Y (2013) A high-performance supercapacitor-battery hybrid energy storage device based on graphene-enhanced electrode materials with ultrahigh energy density. Energy Environ Sci 6:1623–1632. https://doi.org/10.1039/C3EE40509E

Zhang J, Shi Z, Wang C (2014a) Effect of pre-lithiation degrees of mesocarbon microbeads anode on the electrochemical performance of lithium-ion capacitors. Electrochim Acta 125:22–28. https://doi.org/10.1016/j.electacta.2014.01.040

Zhang W, Lin H, Kong H, Lu H, Yang Z, Liu T (2014b) High energy density PbO_2/activated carbon asymmetric electrochemical capacitor based on lead dioxide electrode with three-dimensional porous titanium substrate. Int J Hydrogen Energ 39:17153–17161. https://doi.org/10.1016/j.ijhydene.2014.08.039

Zhao X, Johnston C, Grant PS (2009) A novel hybrid supercapacitor with a carbon nanotube cathode and an iron oxide/carbon nanotube composite anode. J Mater Chem 19:8755–8760. https://doi.org/10.1039/B909779A

Zhao M-Q et al (2015a) Flexible MXene/carbon nanotube composite paper with high volumetric capacitance. Adv Mater 27:339–345. https://doi.org/10.1002/adma.201404140

Zhao MQ et al (2015b) Flexible MXene/carbon nanotube composite paper with high volumetric capacitance. Adv Mater 27:339–345. https://doi.org/10.1002/adma.201404140

Zhou L et al (2017) Cubic Prussian blue crystals from a facile one-step synthesis as positive electrode material for superior potassium-ion capacitors. Electrochim Acta 232:106–113. https://doi.org/10.1016/j.electacta.2017.02.096

Zhu J et al (2014) 3D carbon/cobalt-nickel mixed-oxide hybrid nanostructured arrays for asymmetric supercapacitors. Small 10:2937–2945. https://doi.org/10.1002/smll.201302937

Zhu Y, Yang Y, Fu L, Wu Y (2017) A porous gel-type composite membrane reinforced by nonwoven: promising polymer electrolyte with high performance for sodium ion batteries. Electrochim Acta 224:405–411. https://doi.org/10.1016/j.electacta.2016.12.030

Zuo W, Li R, Zhou C, Li Y, Xia J, Liu J (2017) Battery-supercapacitor hybrid devices: recent progress and future prospects. Adv Sci 4:1600539. https://doi.org/10.1002/advs.201600539